Renewable and Sustainable Energy Reviews 121 (2020) 109594

Contents lists available at ScienceDirect

Renewable and Sustainable Energy Reviews

journal homepage: http://www.elsevier.com/locate/rser

Spatial and temporal variation in the value of solar power across United States electricity markets

Patrick R. Brown [a,*], Francis M. O'Sullivan [a,b]

[a] Energy Initiative, Massachusetts Institute of Technology, Cambridge, MA, 02139, USA
[b] Lincoln Clean Energy, LLC, Chicago, IL, 60611, USA

ARTICLE INFO

Keywords:
Solar energy
Photovoltaics
Value of solar
Locational marginal price
Distributed energy resources
Merit order effect
Air pollution
Capacity value
Resource adequacy

ABSTRACT

The cost of utility-scale photovoltaics (PV) has declined rapidly over the past decade. Yet increased renewable electricity generation, decreased natural gas prices, and deployment of emissions-control technology across the United States have led to concurrent changes in electricity prices and power system emissions rates, each of which influence the value of PV electricity. An ongoing assessment of the economic competitiveness of PV is therefore necessary as PV cost and value continue to evolve. Here, we use historical nodal electricity prices, capacity market prices, marginal power system emissions rates of CO_2 and air pollutants, and weather data to model the energy, capacity, health, and climate value of PV electricity at over 10 000 locations across six U.S. Independent System Operators (ISOs) from 2010 to 2017. On the energy and capacity markets, transmission congestion in some locations and years results in PV revenues that are more than double the median across the relevant ISO. While the marginal public health benefits from avoided SO_2, NO_x, and $PM_{2.5}$ emissions have declined over time in most ISOs, monetizing the health benefits of PV generation in 2017 would increase median PV energy revenues by 70% in MISO and NYISO and 100% in PJM. Given 2017 PV costs, electricity prices, and grid conditions, PV breaks even at 30% of modeled locations on the basis of energy, capacity, and health benefits, at 75% of modeled locations with the addition of a 50 $/ton CO_2 price, and at 100% of modeled locations with a 100 $/ton CO_2 price. These results suggest that PV cost decline has outpaced value decline over the past decade, such that in 2017 the net benefits of utility-scale PV outweigh the cost at the majority of modeled locations.

1. Introduction

Solar photovoltaics (PV) have demonstrated impressive reductions in cost and increases in deployment over the last decade: From 2010 to 2017, utility-scale system costs fell from 6 $/$W_{ac}$ to < 1.5 $/ W_{ac} and worldwide deployment increased from 40 GW to >400 GW [1,2]. Yet numerous studies have noted that as the deployment of PV (or other zero-marginal-cost generation sources such as wind) increases, the value of PV electricity tends to decline as PV displaces higher-cost generators on the margin and reduces the wholesale price of electricity [3–6]. This

Abbreviations: AC, alternating current; C, Celsius; c-Si, crystalline silicon; CAISO, California Independent System Operator; CC, Pearson correlation coefficient; CF, capacity factor; CO_2, carbon dioxide; DC, direct current; DHI, diffuse horizontal irradiance; DNI, direct normal irradiance; EASIUR, Estimating Air pollution Social Impact Using Regression model; eGRID, Emissions & Generation Resource Integrated Database; EIA, U.S. Electricity Information Administration; EPA, U.S. Environmental Protection Agency; ERCOT, Electric Reliability Council of Texas; FERC, U.S. Federal Energy Regulatory Commission; GHG, greenhouse gas; GHI, global horizontal irradiance; GW, gigawatt; IQR, inter-quartile range; ISO, Independent System Operator; ISONE, Independent System Operator of New England; ITC, investment tax credit; km, kilometer; kW, kilowatt; LCOE, levelized cost of energy; LMP, locational marginal electricity price; LOLE, loss-of-load expectation; m, meter; MACRS, Modified Accelerated Cost Recovery System; MAE, mean absolute error; MBE, mean bias error; μg, microgram; μm, micrometer; min, minute; MISO, Midwest Independent System Operator; MW, megawatt; MWh, megawatt-hour; NO_x, nitrogen oxides; NPV, net present value; NREL, National Renewable Energy Laboratory; NSRDB, National Solar Radiation Database; NYISO, New York Independent System Operator; PJM, Pennsylvania-New Jersey-Maryland Interconnection; $PM_{2.5}$, 2.5 μm-diameter particulate matter; POA, plane-of-array; PPA, power purchase agreement; PV, photovoltaic; RGGI, regional greenhouse gas initiative; rMBE, relative mean bias error; RMSE, root mean square error; rRMSE, relative root mean square error; SI, supplementary information; SO_2, sulfur dioxide; TMY, typical meteorological year; U.S., United States of America; USD, U.S. dollars; VF, value factor; VSL, value of a statistical life; W, watt; WACC, weighted average cost of capital; WECC, Western Electricity Coordinating Council; yr, year.

* Corresponding author.
E-mail address: prbrown@mit.edu (P.R. Brown).

https://doi.org/10.1016/j.rser.2019.109594
Received 19 June 2019; Received in revised form 16 October 2019; Accepted 12 November 2019
Available online 26 December 2019

"merit-order effect" is most pronounced during times of day when solar energy generation is highest, causing the average market value of solar electricity to decline even more rapidly than the average electricity price [7–9]. At the same time, the adoption of emissions-control technology for coal generation over the last decade has reduced the marginal public health benefits of PV capacity [10], and continued decarbonization of the power sector will further reduce these marginal benefits.

A number of strategies have been explored for mitigating the observed and projected value decline of variable renewables at the system level, including long-distance geographic aggregation [11], incorporation of energy storage and price-responsive demand [11,12], and use of high-capacity-factor system designs [13,14]. Additional analyses have shown that siting renewables in locations with high electricity prices [15,16] or high power-system emissions rates [17–19] can lead to larger benefits than siting in locations with the highest capacity factor. Some studies quantify the levelized cost of electricity (LCOE) of PV [20,21] but do not assess variation in the value of solar electricity (sometimes referred to as the levelized avoided cost of electricity [22]). Others address the relative benefits and costs of PV generation at the transmission [23] or distribution level [19,24,25], albeit with coarse spatial resolution and for a limited subset of historical electricity price years. The significant variability in prices and emissions rates within and across electricity markets, the effects of different market structures (particularly related to resource adequacy, i.e. capacity), and the large shifts in emissions rates and prices over the last decade have yet to be synthesized into a consistent framework that captures the spatial and temporal variation in the value of PV.

In this work we address the overarching question: How has the declining cost of PV aligned with changing conditions on the U.S. grid, and what does that imply for the competitiveness of PV today? More specifically: If a marginal addition of solar capacity had been installed at the site of a locational marginal electricity price (LMP) node in a given year between 2010 and 2017, what benefits would it have provided in terms of displaced energy, capacity, public health, and climate change

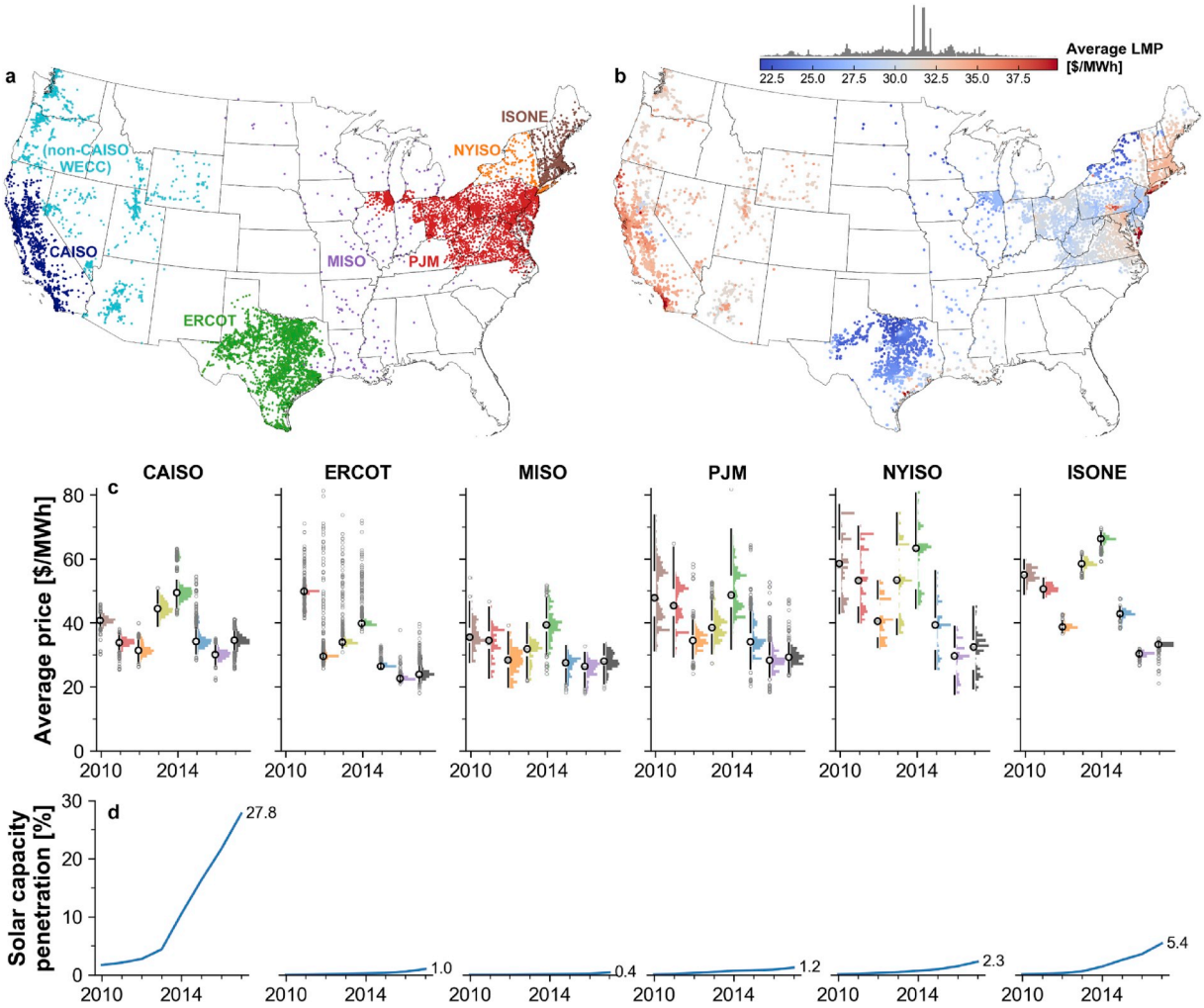

Fig. 1. Variation in locational marginal electricity price (LMP) and solar penetration over the time period analyzed. a, Map of all pricing nodes considered in this study, with the corresponding ISO for each node indicated by the node color [26–29]. Nodes labeled "non-CAISO WECC" lie outside of the CAISO system territory but have LMP and geographic data reported by CAISO. LMP data for a given node are not necessarily available for all years. **b**, Map of average nodal LMP on the day-ahead wholesale market in 2017 [30–36]. **c**, Yearly statistics for day-ahead nodal LMP by ISO for 2010–2017. **d**, Solar capacity penetration for each ISO between 2010 and 2017, given by cumulative installed solar generation capacity (utility-scale and distributed) divided by peak electricity demand within the ISO in each year. Data are from EIA, OpenPV, and the respective ISOs [37,38]. Each column on each subplot in **c** corresponds to a single ISO-year and includes two components: on the left, summary statistics including the median (empty black circle), bootstrapped 95% confidence interval for the median (gray bar), inter-quartile range (IQR, 25 %–75%; white area between black whiskers), whiskers from the edge of the IQR to 1.5 × IQR or the max/min value, whichever is closer (black lines), and outliers beyond the edge of the whiskers (gray circles); on the right, colored 101-bin histograms showing the distribution of values for each ISO-year. Sample sizes for each ISO-year are given in Table SI.1. Y-axis limits for **c** exclude some outlying nodes. (For interpretation of the references to color in this figure legend, the reader is referred to the Web version of this article.)

costs in that year, and what upfront cost would the PV installation have had to achieve to break even over its lifetime, assuming that grid conditions in that year persist for the life of the PV installation?

To answer this question we assemble a large temporally- and spatially-synchronized dataset of historical day-ahead LMPs, system loads, capacity prices, marginal emissions rates and marginal damage rates from power system particulate matter emissions (resulting from SO_2, NO_x, and direct $PM_{2.5}$ emissions), and simulated solar generation, spanning more than 10 000 locations and eight years of operation. We identify significant variation in the value of PV electricity over time and across length scales substantially smaller than the size of Independent System Operators (ISOs). Marginal additions of PV capacity at recent upfront system costs are found to break even at large fractions of nodes for some regions on the basis of energy value, capacity value, and public health benefits alone, and at modest carbon prices for the remainder of locations.

1.1. Analytical approach

Our analysis covers six major U.S. ISOs: California ISO (CAISO), the Electric Reliability Council of Texas (ERCOT), Midwest ISO (MISO), the Pennsylvania-New Jersey-Maryland Interconnection (PJM), New York ISO (NYISO), and ISO-New England (ISONE), with node locations shown in Fig. 1a. At each pricing node for which geographic information and a complete day-ahead LMP timeseries could be obtained for a given year (a sample size ranging from ~7400 nodes in 2010 to ~ 13 700 nodes in 2017, as shown in Fig. SI.1 and Table SI.1), the output of a utility-scale PV generator is simulated using historical irradiance data from the National Solar Radiation Database (NSRDB) [39,40] as inputs to a PV generation model based on the open-source PVLIB toolbox [41,42]. The model accounts for PV module orientation, inverter DC/AC ratio, system and inverter losses, and temperature-induced module efficiency losses. This analysis assumes the use of horizontal 1-axis-tracking crystalline silicon (c-Si) PV arrays with a north/south axis of rotation (tracking from east to west throughout each day) and assumes must-run (i.e. non-curtailable) PV operation. A companion analysis uses this dataset to explore the impact of temporal PV output shaping—through tracking, curtailment, and orientation optimization—on the wholesale market value of PV energy [43].

Modeled PV generation is validated at the monthly timescale against reported generation from hundreds of utility-scale PV plants [37,44], and at the hourly timescale against reported generation from a ~1 MW PV array at the site of the National Renewable Energy Laboratory (NREL) [45]. Full validation results are described in the Supplementary Information (SI Note 3 and Figs. SI.10–SI.19).

At each node we assess four separate components of the value of a modeled PV generator, measured in $\$/kW_{ac}$ per year: energy (from the LMP), capacity (i.e. resource adequacy), public health benefits (arising from the offset of SO_2, NO_x, and $PM_{2.5}$ emissions), and climate change mitigation arising from CO_2 emissions abatement. Capacity revenue is given by combining historical capacity market clearing or contract prices with the calculated "capacity credit" for PV—the amount of firm generation capacity that a unit of PV capacity can displace while maintaining system reliability at the same level, indicating the fraction of the PV unit's peak capacity for which it is compensated on the capacity market. Marginal emissions rates and damages, taken from Azevedo et al. [46], are differentiated geographically by U.S. Environmental Protection Agency (EPA) Emissions & Generation Resource Integrated Database (eGRID) region [47] and temporally by year, hour of day, and season [19]. Marginal emissions rates reflect empirical estimates of the merit-order response of power system dispatch to a change in demand in each hour (here resulting from an increase in PV generation) [17,48], with emissions levels typically falling between the operational emissions rates of natural gas and coal (Fig. SI.6). Monetized public health benefits in Azevedo et al. [46] are calculated using the EASIUR model [49–51], and monetized climate benefits are determined from the marginal emissions offset multiplied by a chosen carbon price. All monetary values are given in 2017 U.S. dollars (inflated from nominal input data using the Consumer Price Index [52]), and electric power and capacity factors are given in terms of AC output from the PV inverter.

2. Methods

2.1. Data sources

Meteorological data: Meteorological data including global horizontal irradiance (GHI, W/m^2), direct normal irradiance (DNI, W/m^2), diffuse horizontal irradiance (DHI, W/m^2), surface air temperature (°C), and surface wind speed at 2 m height (m/s) are taken from the National Solar Radiation Database Physical Solar Model (NSRDB PSM) [39]. These data are derived from satellite observations and are available on a 4 km × 4 km grid across the continental United States, at 30 min resolution for historical data from 1998 to 2017 and at 60 min resolution for a typical meteorological year (TMY). The meteorological data for a given timestamp are assumed to remain constant until the next timestamp; for example, the reported insolation, wind speed, and temperature at 8:00 are assumed to remain constant until 8:30. Historical meteorological data are used for all calculations; Figs. SI.9 and SI.21 show the observed difference between historical and TMY capacity factors.

Electricity price: Complete sets of hourly day-ahead LMP data for electricity at all reported pricing nodes are obtained from the respective ISOs [30–36]. For simplicity, all nodes within California are labeled as "CAISO", even though the CAISO footprint does not cover the entire state of California. Only nodes with serially complete LMP availability for a given calendar year are utilized.

The geographic locations of pricing nodes for CAISO, MISO, PJM, and NYISO are obtained from publicly-available sources. Node latitudes and longitudes for CAISO and MISO are available directly [26,27]. For PJM, node locations are inferred from a list of the closest nodes to each zip code within the PJM service area [28]; the location of each node is taken as the centroid of the centers of all of the zip codes that list that node. For NYISO, node locations are resolved at the city or county level [29]; if a single node is listed for multiple cities or counties, the location of that node is taken as the centroid of the centers of all the cities or counties that list that node. Node locations for ERCOT and ISONE are not publicly available, and were obtained through correspondence with ISO representatives. Only pricing nodes with both LMP and geographic information are used in this analysis. A map of nodal data availability is given in Fig. SI.1.

Capacity market clearing prices are obtained from the respective ISOs [53–57]. Pricing nodes are assigned to capacity zones based on their geographic locations (for MISO [27], NYISO [58], and ISONE) or published node-to-zone listings (for CAISO [26] and PJM [59]).

Load: Hourly load used in the calculation of PV capacity credit is taken from the FERC Form 714 Database [60]. The MISO coverage area has changed over the analyzed time period; MISO load in each year is taken as the sum of loads for MISO, SMEPA (South Mississippi Electric Power Association), Cleco, and Entergy.

Marginal emissions and damages: Marginal emissions rates for CO_2, SO_2, NO_x, and $PM_{2.5}$, and marginal public health damages for SO_2, NO_x, and $PM_{2.5}$, are taken from Azevedo et al. [46] and described in detail in Siler-Evans et al. [17,48]. Emissions rates are disaggregated by EPA eGRID region [47], year, season (Summer, May–September; Winter, November–March; Transitional, April and October), and hour of day. Marginal damages are calculated using the EASIUR model [49–51] assuming a value of a statistical life (VSL) of 8.6 million USD2010 and a relative risk of 1.06 per 10 $\mu g/m^3$ increase in $PM_{2.5}$ concentration. Marginal damages calculated using the AP2 model, which are not used in the analysis but are provided for comparison with results from the EASIUR model, are shown in Fig. SI.36 [46,61–63]

PV capacity: PV capacity penetration in Fig. 1d includes utility-scale

PV capacity reported in EIA Form 860 [37] and distributed PV capacity reported by the OpenPV project [38]. The EIA Form 860 database only includes installations greater than 100 kW in capacity, so to prevent double-counting between the two data sets, only installations with capacity less than 100 kW are included from OpenPV. Capacity penetration is calculated by dividing the sum of utility-scale PV and distributed PV capacity by the peak ISO-wide demand in each year. The DC/AC ratio χ is assumed to be 1 for installations reported in the OpenPV dataset. For the purpose of PV capacity quantification in Fig. 1d, CAISO includes all of California; ERCOT includes all of Texas; PJM includes all of Ohio, Pennsylvania, New Jersey, Delaware, Maryland, West Virginia, and Virginia; MISO includes all of North Dakota, South Dakota, Minnesota, Wisconsin, Iowa, Illinois, Indiana, Michigan, Arkansas, Louisiana, and Mississippi; NYISO includes all of New York; and ISONE includes all of Maine, Vermont, New Hampshire, Massachusetts, Rhode Island, and Connecticut.

2.2. PV generation

2.2.1. Model formulation

Time-resolved alternating-current (AC) PV power generation for a PV generator at each pricing node is simulated using the open-source PVLIB Python toolbox originally developed at Sandia National Laboratories [41,42,64], with input meteorological data taken from NSRDB as described above. Numerical assumptions for PV system characteristics are listed in Table 1. Assumptions generally match those used in the PVWatts model for crystalline silicon modules [65,66] and recent PV industry trends [1,67].

For a given node location, the solar position and extraterrestrial DNI are calculated at each timestamp, and airmass is determined from the calculated solar position. For 1-axis tracking, the tracker angle ψ is calculated at each timestamp from the solar position, axis tilt (θ), and axis azimuth (φ), subject to the maximum tracker angle ψ_{max} and ground coverage ratio κ. "Backtracking"—a reduction in the tracker angle ψ during times close to sunrise and sunset to prevent shading between parallel rows of panels—is employed for all tracking simulations [68]. Direct and diffuse plane-of-array (POA) irradiance are calculated according to the Reindl diffuse sky model [69,70], taking into account the solar position, array orientation, measured irradiance (GHI, DNI, and DHI) from NSRDB, airmass, extraterrestrial DNI [71,72], and ground albedo (which contributes to diffuse POA irradiance at nonzero tilt angles). Off-normal reflection losses for direct POA irradiance are calculated from Fresnel's equation as in Ref. [65] assuming indexes of refraction $n_{air} = 1$ for air, n_{ar} given in Table 1 for the antireflection coating, and $n_{glass} = 1.526$ for glass. Global POA irradiance is calculated from the sum of direct (after reflection losses), sky diffuse, and ground diffuse POA irradiance. PV cell temperature is calculated using the Sandia PV Array Performance Model [73] assuming open rack mounting with polymer backplane modules, taking into account surface air temperature and wind speed from NSRDB and global POA irradiance. DC power output as a fraction of nameplate DC capacity P_{dc}^0 is given by

$$\frac{P_{dc}}{P_{dc}^0} = \frac{I_G^{POA}}{1000}\left(1 + \gamma(T_{cell} - 25^{\circ}\mathrm{C})\right)\left(1 - \eta_{system}\right) \quad (1)$$

where I_G^{POA} is global POA irradiance (W/m^2), γ is the temperature coefficient of the PV cell, T_{cell} is the calculated PV cell temperature, and η_{system} is the DC system losses. AC power output as a fraction of nameplate AC capacity is calculated as in PVWatts [65] incorporating the DC/AC ratio χ and nominal inverter losses $\eta_{inverter}$. When $(P_{dc}/P_{dc}^0) \times \chi > 1$, the AC output is clipped to the nameplate AC capacity. Fig. SI.8 in the Supplementary Information shows the sensitivity of calculated AC capacity factor to changes in each of the variables listed in Table 1.

Table 1
Default assumptions for PV generation model.

Parameter	Symbol	Value	Units
Axis tilt, 1-axis tracking array	θ	0	degrees from horizontal [°]
Axis azimuth	φ	180	degrees clockwise from north [°]
DC/AC ratio	χ	1.3	fraction [.]
DC system losses	η_{system}	14	percent [%]
Nominal inverter losses	$\eta_{inverter}$	4	percent [%]
Temperature coefficient	γ	−0.4	percent relative to 25°C [%/°C]
Maximum tracker angle	ψ_{max}	60	degrees from center [°]
Ground coverage ratio	κ	0.33	fraction [.]
Ground albedo	β	0.2	fraction [.]
Antireflection coating index	n_{ar}	1.3	fraction [.]

2.2.2. Model validation

To assess the accuracy of the PV generation model and the suitability of the model assumptions noted above, modeled PV capacity factors are validated against two sets of empirical data: monthly reported generation from hundreds of utility-scale PV plants from the EIA Form 860 [37] and Form 923 [44] databases; and hourly reported generation for a single PV installation from the PVDAQ database [45]. Monthly validation is relevant for assessing the accuracy of PV revenue calculations, which scale with capacity factor; hourly validation is additionally relevant for average value and value factor calculations, which depend on the temporal profile of PV generation throughout each day.

Monthly validation: The EIA Form 860 database includes information on plant location, nameplate AC capacity, installation date, and technical design parameters for every utility-scale power plant in the U.S. For PV plants, these data include PV module technology, array tilt angle (θ), tracking strategy employed, and nameplate DC capacity (which, when divided by the nameplate AC capacity, gives the DC/AC ratio χ). The EIA Form 923 database reports monthly electricity generation for the majority of the plants included in the EIA 860 database. For each PV plant shared between the Form 860 and Form 923 databases, we simulate the plant capacity factor using the reported system parameters and historical insolation at the site of the plant and compare the simulated results (averaged over each calendar month) with the historical reported monthly generation of the plant over the years 2014–2016. The data are subsetted to include only those plants with DC/AC ratio between 0.5 and 2.5 and either a single fixed-tilt orientation or one-axis tracking; dual-axis-tracking plants, plants employing concentration or multiple orientations, and plants lacking orientation data are dropped from the sample. All 1-axis tracking installations are assumed to have $\theta = 0^{\circ}$. Plants with less than 0.1 MWh of reported generation in any month of a given year and plants with an annual reported capacity factor of less than 5% for a given year are also dropped from the sample, as well as plants with less than a full year of operation for any given year. The cleaned validation dataset includes 542 plants for 2014, 800 plants for 2015, and 1170 plants for 2016. The temperature coefficient γ is assumed to be −0.4%/°C for plants employing crystalline silicon PV modules and −0.2%/°C for plants employing thin-film PV modules. Other simulation parameters not reported in the Form 860 database are taken from Table 1.

Figs. SI.10–SI.12 in the Supplementary Information display the locations of the plants in the validation set and reported and simulated generation for 2014–2016. Simulation accuracy is assessed in terms of the Pearson correlation coefficient (CC), mean absolute error (MAE), mean bias error (MBE), relative mean bias error (rMBE), root mean square error (RMSE), and relative root mean square error (rRMSE) between the monthly simulated and reported capacity factor for each plant in each year. Validation metrics are displayed in Figs. SI.13–SI.15 and discussed in SI Note 3.

Hourly validation: The PVDAQ database includes time-resolved power generation data for over 100 PV installations across the U.S., with varying levels of detail regarding the system design parameters for each installation. We select system number 1332, a 1.135 MW$_{ac}$ fixed-

tilt PV array at the site of the National Renewable Energy Laboratory, for hourly validation purposes, as it is the largest array in the database and includes data on system azimuth (180°), tilt (16.8°), and DC/AC ratio (1.02). Hourly validation results are discussed in SI Note 3; Figs. SI.16 and SI.17 display simulated and measured PV output for the validation site over the years 2014–2016, and Figs. SI.18 and SI.19 display simulation accuracy statistics (CC, MAE, MBE, rBME, RMSE, and rRMSE) binned by month and by hour of day.

2.3. Energy, capacity, and emissions abatement value

2.3.1. Wholesale energy value

Annual energy revenue R^{energy} in $/kW$_{ac}$ per year for a PV generator at a given node is given by

$$R^{energy} = \sum_{t=0}^{N} \frac{P_t}{P_{max}} \Pi_t \left(\frac{\tau}{60}\right) \tag{2}$$

where t is a timestamp, N is the number of timestamps in the year (e.g. 17520 for 30 min timestamps in a non-leap year), P_t is the modeled AC power output of the PV system in timestamp t, P_{max} is the peak AC power output of the PV system, Π_t is the LMP in timestamp t, and τ is the period of the timestamp in minutes (i.e. 30 min for historical PV output). As the native period of the LMP (60 min) is longer than that of the modeled PV output (30 min), the LMP is resampled to match the period of the PV output, with new timestamps taking the value at the most recent existing timestamp (i.e. forward-filled).

The average value of PV electricity V in $/MWh at a given node is given by

$$V = \frac{\sum_{t=0}^{N} P_t \Pi_t}{\sum_{t=0}^{N} P_t}. \tag{3}$$

The PV value factor VF at a given node indicates the ratio between the average value of PV electricity V and the average price of electricity at that node:

$$\mathrm{VF} = \frac{V}{\overline{\Pi}} = \left(\frac{\sum_{t=0}^{N} P_t \Pi_t}{\sum_{t=0}^{N} P_t}\right) \times \frac{N}{\sum_{t=0}^{N} \Pi_t}. \tag{4}$$

2.3.2. Capacity value

The capacity credit of PV can be calculated using a number of different methods [74–78]. The most rigorous method is to calculate the system-wide loss of load expectation (LOLE) following the addition of the specific PV generator, then to determine the equivalent capacity of a conventional firm generator that, if added to the system in place of the PV generator, would result in the same LOLE [77]. This calculation requires a large amount of system- and generator-specific operational data. A commonly-used approximation method with fewer data requirements, which has historically been used by MISO, PJM, NYISO, and ISONE in addition to several studies in the literature [15,75,76,79–81], is to identify the capacity credit as the capacity factor of the PV generator during a specified subset of (typically high-load or high-loss-of-load-probability) hours over a given time period. Here we use the capacity-factor approximation method, which has been shown to agree reasonably well with the more rigorous LOLE-based method for PV [82].

PV capacity credit ξ for a given node and year is given by

$$\xi = \frac{\sum_{t=0}^{N} \alpha_t P_t}{\sum_{t=0}^{N} \alpha_t P_{max}}, \tag{5}$$

where α_t is 1 if t is a critical-load hour and 0 otherwise. Two different rules for identifying critical-load hours α_t are used here. In the *peak net-load* method, a specified percentage of hours with the highest net load are labeled as critical, where net load is ISO-wide demand minus simulated utility-scale solar generation and ISO-reported wind generation (where available) in the specified year. ISO-wide solar generation is simulated as described above for purposes of monthly model validation, using utility-scale solar plant locations and system parameters from the EIA Form 860 database [37] for plants located with each ISO boundary. Hourly wind generation is taken from the respective ISOs, and is available since 2010 for ERCOT and MISO and since 2011 for CAISO, ERCOT, and PJM [32,33,83–86]. For NYISO and for years outside these ranges, wind is ignored and net load is taken as demand minus solar generation. Figs. SI.32 and SI.33 show the capacity credit under different peak-hour thresholds and load assumptions.

In the *ISO-specified* method, critical hours are defined by the ISOs as follows:

- MISO: Hours beginning at 2pm, 3pm, 4pm from June–August (276 h) [87].
- PJM: Hours beginning at 2pm, 3pm, 4pm, 5pm from June–August (368 h) [88].
- NYISO: Hours beginning at 2pm, 3pm, 4pm, 5pm from June–August, and hours beginning at 4pm, 5pm, 6pm, 7pm from December–February (728 h in a non-leap year) [89].
- ISONE: Hours beginning at 1pm, 2pm, 3pm, 4pm, 5pm in June–September, and hours beginning at 5pm, 6pm in October–May (1096 h in a non-leap year) [90].

For both methods, the capacity credit for a given node and year is calculated using modeled PV generation during the specified year. Some ISOs and literature studies [81,91] use multiple years of operational data to calculate PV capacity credit; here, for consistency across ISOs and to maintain any historical correlation between PV availability and net load, we use the production profile P_t for a single year to assess the capacity credit and revenue for that year. Modeled nodal PV output P_t at 30 min resolution is downsampled via trapezoidal integration to match the 60 min resolution of system load and wind generation (e.g. PV output for the 8:00 bin is given by the integral of PV output between 8:00–9:00).

PV capacity revenue $R^{capacity}$ ([$/kW$_{ac}$ per year]) is given by

$$R^{capacity} = \frac{\sum_{t=0}^{N} \alpha_t P_t \Pi_t^{capacity}}{\sum_{t=0}^{N} \alpha_t P_{max}}, \tag{6}$$

where $\Pi_t^{capacity}$ is the historical capacity price in $/kW$_{ac}$ per year. Capacity prices are defined over different intervals across the different ISOs: for CAISO, capacity prices are defined by calendar year (January 1–December 31); for MISO, PJM, and ISONE, capacity prices are defined from June 1–May 31; for NYISO, capacity prices are defined by season (May 1–October 31 for summer and November 1–April 30 for winter). If the capacity price is defined by calendar year (e.g. for CAISO), equation equation (6) simplifies to $R^{capacity} = \xi \Pi^{capacity}$.

2.3.3. Emissions mitigation

The annual marginal CO_2 emissions abatement M_{CO_2} in ton/kW_{ac}$ per year at a given node is given by

$$M_{CO_2} = \sum_{t=0}^{N} \frac{P_t}{P_{max}} m_t \tag{7}$$

where m_t is the hourly marginal CO_2 emissions rate in the eGRID region containing the node. Annual marginal abated public health cost H in $/$kW$_{ac}$ per year at a given node is given by

$$H = \sum_{z \in [SO_2, NO_x, PM_{2.5}]} \sum_{t=0}^{N} \frac{P_t}{P_{max}} h_t^z \tag{8}$$

where h_t^z is the hourly marginal damage rate of species z in the eGRID region containing the node.

2.4. Limitations of this analysis

We note the following caveats and limitations before describing our results.

- The PV system services considered here include a combination of private benefits (resulting from market earnings from the LMP and capacity market) and public benefits (from air pollution and greenhouse gas mitigation) [92]; unless clearly stated otherwise, we do not include the impact of explicit subsidies (such as the investment tax credit or renewable energy credits procured to meet renewable portfolio standards) or implicit subsidies (such as net energy metering), which would entail a public-to-private wealth transfer from taxpayers and ratepayers to the solar owner. There are two potential interpretations within which the private and public benefits considered here can be put on equal footing. The first interpretation is to consider these values in a hypothetical policy environment where market-based policies capture the external cost of emissions, such that the total revenues calculated here are equivalent to private monetary gains by the solar owner. The second interpretation is from the point of view of a centralized power system planner. In this interpretation all benefits are public; net revenue represents the net benefit to society of avoided expenditures for energy and capacity provision and realized public health and climate benefits. We note that PV can result in further benefits and costs on the distribution system, including impacts (positive and negative) on distribution system losses, congestion, and upgrade requirements or deferral [93]. These factors have been explored in other studies [94–96], but require significantly more data on distribution system structure than is publicly available from the ISO sources used here.
- As we take the historical LMPs, loads, and marginal emissions rates as fixed, our results are relevant for assessing how a marginal unit of PV capacity—a "price-taker" in the context of the energy and capacity markets—competes with existing incumbent generators, and the impact of replacing existing generation with new PV generation. In the framework of Lamont [4] and Baker et al. [97], we thus address the "short-run" value of solar, as opposed to the medium- or long-run value, where the generation mix and associated price of electricity would be allowed to respond to additions of solar capacity. If a significant amount of PV generation capacity is installed at a given node or within the node's balancing area, LMPs and the value of PV electricity at that location, as well as the PV capacity credit and marginal emissions offset, would decline due to the merit-order effect noted above. Other studies have employed econometric methods to assess the degree of causal relationship between solar deployment and solar value decline at the level of states or ISOs [98–100]; the data presented here could be used to increase the spatial resolution of such studies in subsequent work.
- We do not consider the impact of solar forecasting for participation in the day-ahead market; in effect we assume that the hourly day-ahead availability of each PV generator is perfectly predictable. A real PV plant would likely balance its participation in the day-ahead and real-time markets based on its confidence in output forecasts, expected divergence between day-ahead and real-time prices, and the magnitude of penalties imposed for deviation from scheduled generation. We also note that while most utility-scale PV plants sign multi-year power purchase agreements (PPAs) rather than rely solely on market revenues, the PPA value should scale with changes in the market value in a competitive market (with additional adjustments from applicable subsidies and the value of electricity price hedging, which are not included here).
- In the quantification of climate impacts, we only consider operational emissions of CO_2, in keeping with the implementation of contemporary CO_2 taxation and cap-and-trade schemes. In a complete lifecycle assessment, both PV and the marginal generation sources displaced by PV (primarily natural gas and coal, with the time-varying mix of displaced generation accounted for in the marginal emissions data used here) are responsible for additional non-operational emissions associated with component manufacture, plant construction, and, in the case of fossil-fired generation, fuel extraction and transport. Recent studies report that the levelized non-operational greenhouse gas emissions (GHG) of PV installed in the U.S. are lower than non-operational emissions for coal and natural gas [101,102]. Quantifying GHG emissions in a lifecycle (rather than operational) framework would thus increase the modeled value of PV for climate change mitigation. The inclusion of additional environmental and health effects besides the CO_2 and particulate matter impacts included here (including human toxicity, aquatic and terrestrial ecotoxicity, and freshwater eutrophication) would further increase the value of PV [102].
- The monetized health and climate benefits assessed here are sensitive to assumptions, particularly regarding the value of a statistical life (VSL) and discount rate. Climate benefits are difficult to quantify given the presence of positive and negative feedbacks, nonlinear tipping points, and the intergenerational nature of climate impacts [103], and the appropriateness of using cost-benefit analysis to assess environmental impacts or existential risks such as climate change is open to debate [104,105]. We do not assert that the prices assumed here for abated health and climate damages are the "right" prices; we simply explore the implications of assuming values widely used in the literature [10,17]. The quantitative values of our results will change for different assumptions regarding these prices, but the directionality of the trends will be the same. The impact of alternative assumptions on the results presented here can be explored using the open-source computer code provided in the "Data and computer code availability" section.
- The presence of an emissions cap and trade program can complicate an assessment of the marginal emissions offset of solar. Under a firmly binding cap, a ton of emissions offset by new solar generation would be replaced by a ton of emissions from another source. There are two cap and trade programs for carbon emissions active in the regions explored here: the California cap and trade program, and the Regional Greenhouse Gas Initiative (RGGI) for Connecticut, Delaware, Maine, Maryland, Massachusetts, New Hampshire, New Jersey, New York, Rhode Island, and Vermont (covering all of ISONE and NYISO and part of PJM). As shown in Fig. SI.3, over the time period analyzed, market clearing prices for CO_2 have been low: less than 15 $/ton for California (within $3 of the floor price in all years) and less than 7 $/ton for RGGI in all years [106,107]. SO_2 emissions are also subject to a cap and trade program under the EPA Acid Rain Program, but prices have been consistently low over the time period analyzed: 42 $/ton in 2010 and 3 $/ton or less in subsequent years, compared to a maximum of 1074 $/ton in 2006 and a median public health cost ranging from 8000 $/ton to 47000 $/ton over the regions and time period analyzed [46,108]. For the assessment of the climate benefits of a marginal unit of PV generation, we subtract the clearing price for CO_2 in the California cap and trade program and RGGI for nodes covered by these markets from the applied carbon price, as the clearing price is already factored into the LMP value. Effectively we negate the effect of existing cap and trade regulations on energy prices, then re-apply a uniform hypothetical carbon price across the ISOs. We do not model the effects of a higher carbon price on the merit-order dispatch stack; if formally implemented, a higher carbon price would make lower-emissions generators more likely to be dispatched, thus decreasing the marginal emissions rate of CO_2 and other pollutants and decreasing the emissions benefit of PV. No correction is made for the market clearing price of SO_2 given the very low price of SO_2 allowances over the time period analyzed compared to the social cost.

3. Components of the value of PV electricity

3.1. PV energy value

Fig. 2a displays a map of the modeled yearly energy revenue for PV arrays on the day-ahead wholesale market in 2017, and Fig. 2b and c displays trends in revenue and value factor differentiated by ISO for each year from 2010 to 2017. Maps of the spatial distribution of revenue and value factor for each year, as well as maps and trends for the average value of solar electricity in $/MWh, are displayed in Figs. SI.23–SI.25 in the Supplementary Information.

It is notable that the sunniest locations are not always the most profitable locations to install solar: the median nodal LMP revenue in the northeast (ISONE and NYISO) is greater than the median nodal LMP revenue in Texas (ERCOT) in three out of the seven years analyzed, despite the ~20% higher median PV capacity factor in ERCOT. Two observations indicate that variation in solar revenue between sites is dictated more by variation in nodal LMP than by variation in capacity factor. First, the yearly variability in revenue (Fig. 2b) is much greater than yearly variability in capacity factor (Fig. SI.20a): median revenues over all ISOs and nodes range from 67 $/kW$_{ac}$ per year in 2017 to 110 $/kW$_{ac}$ per year in 2014 (a 65% difference), while median capacity factors range from 22.5% in 2011 to 24.7% in 2016 (a 10% difference) and median LMPs range from 28.1 $/MWh in 2016 to 48.5 $/MWh in 2014 (a 73% difference). Second, spatial trends in yearly revenue (Fig. 2a) more closely match spatial trends in average LMP than capacity factor (Fig. 1b, Fig. SI.21), and variance arising from congestion is larger than variance arising from capacity factor in most of the ISOs analyzed

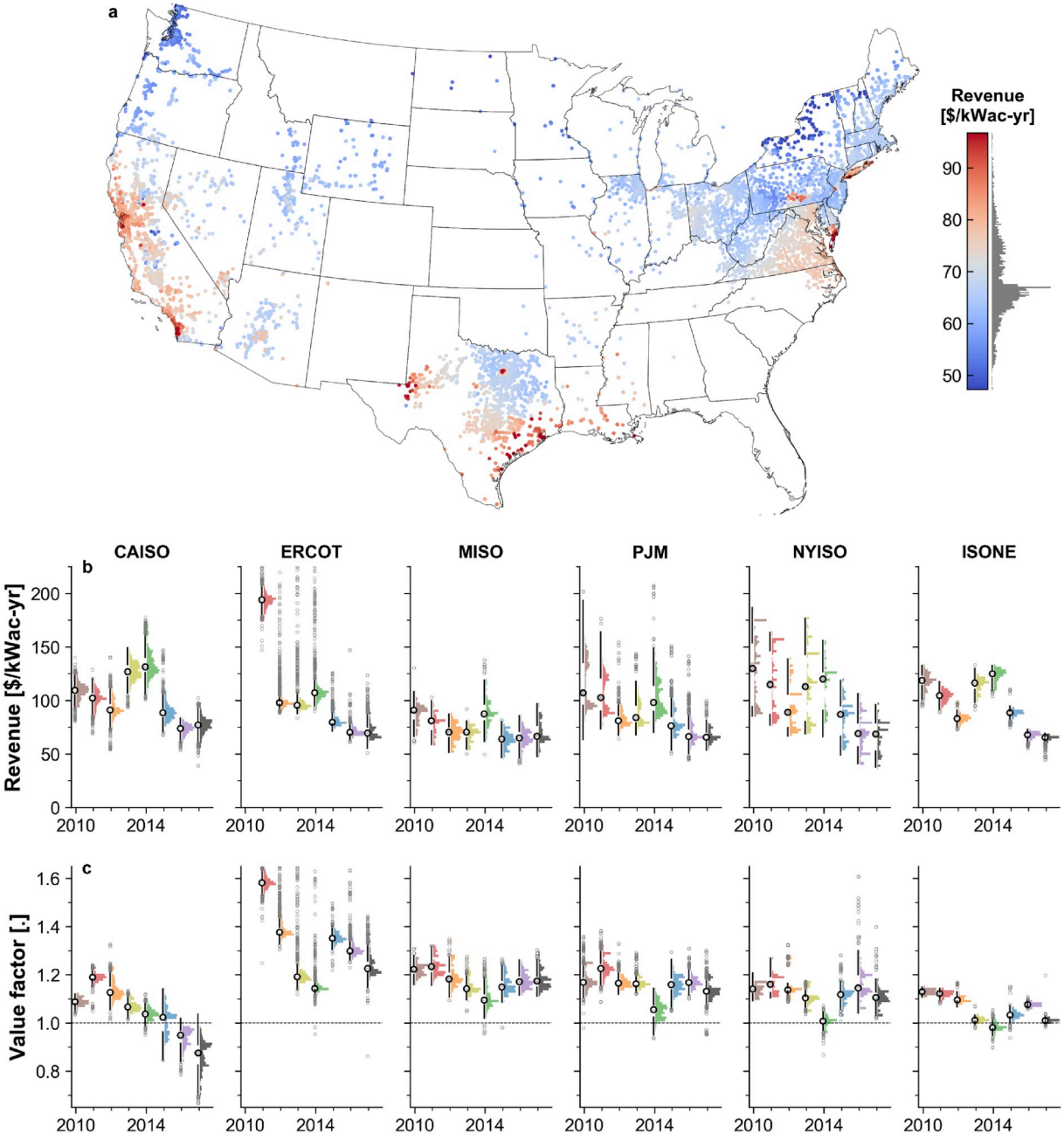

Fig. 2. Modeled yearly PV revenue (a) on the day-ahead wholesale electricity market in 2017, and yearly statistics for PV revenue (b) and value factor (c) by ISO for 2010–2017. Each marker in **a** represents one pricing node. Statistics in **b-c** are displayed in the same format as Fig. 1c. The value factor is the ratio of the average value of a MWh of solar electricity to the average price of electricity over the year.

(Fig. SI.30). These effects manifest most strongly in the observation of "hotspots" within the PJM ISO along the east coast where the yearly solar revenue is in some years more than double the median across the ISO as a whole.

While we focus on the years 2010–2017 for the bulk of this study given more complete data coverage across all ISOs for these years, PJM and NYISO provide LMP data dating back to 2001 and 2000, respectively. As shown in Figs. SI.26–SI.28, the hotspots noted above, particularly on Long Island and the Delmarva peninsula, have been observed for more than a decade, and the same collection of nodes tend to remain at the high extreme of the nodal revenue distribution from year to year. Disaggregation of the LMP into the marginal costs of energy, congestion, and losses (Figs. SI.29–SI.31) shows that these hotspots are driven by high congestion prices, which increase wholesale market revenues by more than 50 $\$/kW_{ac}$ per year for some years. While the observed revenue dispersion is long-lived, the magnitude of the revenue at these nodes tends to rise and fall in line with trends in the ISO median revenue, driven by year-to-year variation in the energy price.

There is also notable variation in value factor between the different ISOs. ERCOT demonstrates the highest median value factor in each year

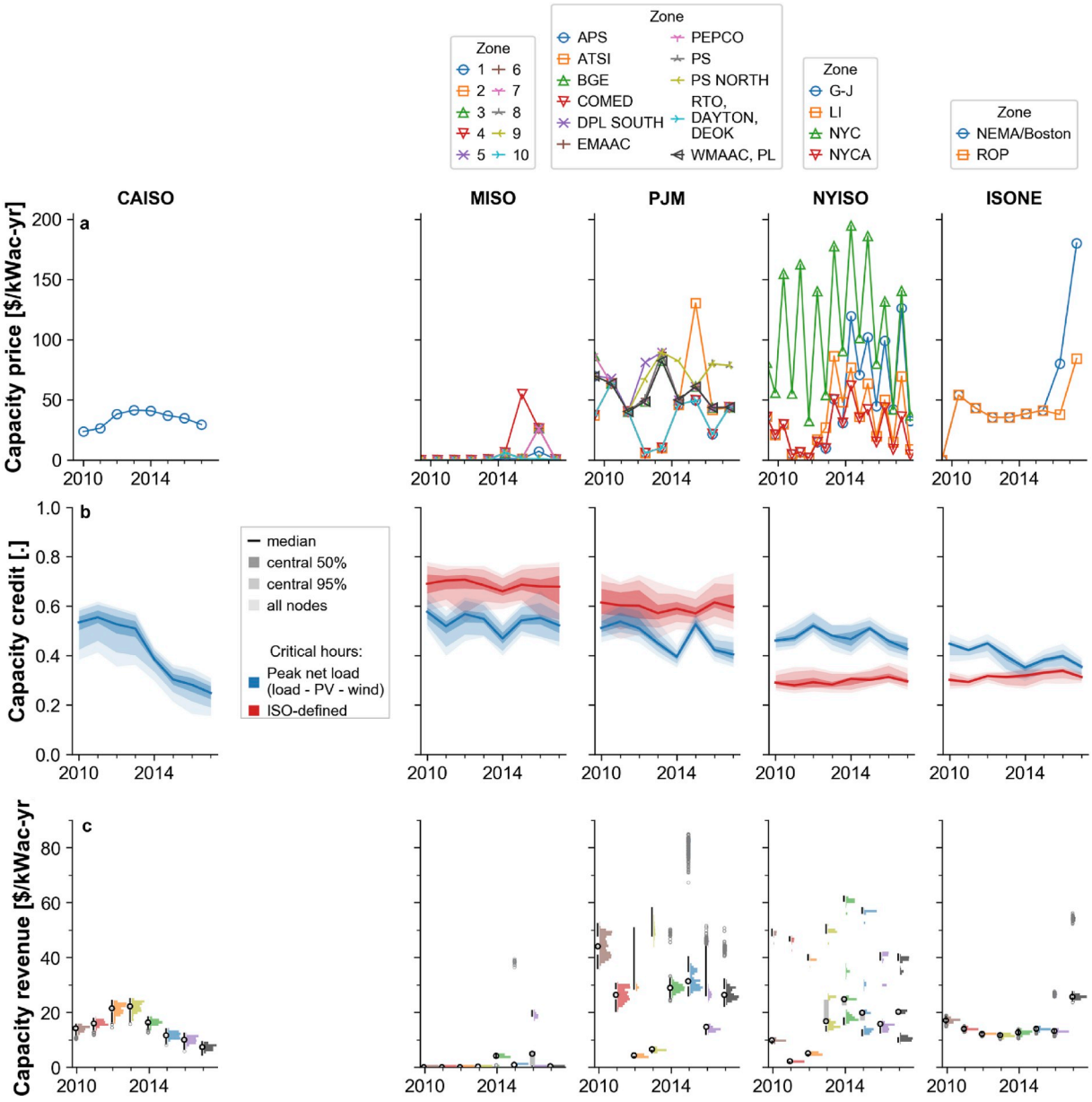

Fig. 3. Capacity value of PV by ISO. a, Historical capacity price by ISO resource-adequacy zone [53–57]. Zone maps are shown in Fig. SI.7 in the Supplementary Information. Prices for CAISO are weighted average (median for 2010–2011 due to data availability) capacity contract prices; prices for MISO, PJM, NYISO, and ISONE are market-clearing prices. ERCOT is not included in this analysis as it does not have a capacity market. Intervals before the capacity market became active in a given ISO (before the 2010/2011 season in ISONE and before the 2013/2014 season in MISO) are assigned a price of zero. Data for CAISO, MISO, PJM, and ISONE reflect annual capacity auction prices, while data for NYISO include both summer and winter capacity auction prices. Markers are located at the beginning of the corresponding compliance period; lines between markers are guides to the eye. **b**, Distribution of modeled PV capacity credits across all nodes in each ISO from 2010 to 2017, given by the average capacity factor of a modeled 1-axis-tracking PV array during "critical-load hours" over each year. Red curves indicate capacity credit calculated assuming ISO-specified critical-load hours; blue curves indicate capacity credit calculated with the top 7.04% of net load hours (ISO-wide demand minus modeled utility-scale solar and ISO-reported wind production) taken as critical-load hours. **c**, Distribution of modeled PV capacity revenues by ISO over time for PV arrays at all modeled ISO nodes. Revenues are calculated using the top 7.04% of net load hours for CAISO and the ISO-specified hours for MISO, PJM, NYISO, and ISONE. (For interpretation of the references to color in this figure legend, the reader is referred to the Web version of this article.)

(Fig. 2c); given ERCOT's low solar penetration, high air conditioning load during sunny periods, and high price cap for electricity (associated with ERCOT's unique status as the only "energy-only" electricity market among the ISOs considered here), PV generation is likely to coincide with high-price periods in the ERCOT system, increasing its value factor. CAISO demonstrates the most pronounced decline in value factor over the period studied—from a median value factor of 1.09 in 2010 (1.06–1.12 at the central 95% of nodes) to 0.87 in 2017 (0.72–0.96 at the central 95% of nodes)—coinciding with its 15× increase in solar capacity penetration over this time period (Fig. 1d).

3.2. PV capacity value

In markets where the LMP is administratively capped at an upper limit, additional payments to generators are necessary to ensure that there is adequate incentive to install sufficient generation capacity to meet demand across all hours. These "capacity payments" are made either through bilateral contracts between grid operators and individual generators (in the case of CAISO), or through a capacity market that clears seasonally or yearly (in the case of MISO, PJM, NYISO, and ISONE). Fig. 3a shows the historical capacity prices for the five ISO capacity markets considered here [53–57], and Fig. 3b shows the nodal distribution of calculated capacity credits for 1-axis-tracking PV over 2010–2017. Where possible, capacity credits are shown using both ISO-defined critical hours (red curves) and the highest 7.04% of net-load hours (blue curves) per year, where 7.04% is the average of the number of hours used by MISO, PJM, NYISO, and ISONE for PV capacity credit assessment [87–90].

As shown in Fig. 3b and Fig. SI.33 and noted in Refs. [75,82], the capacity credit is sensitive to the number of hours counted as critical; in general the higher the number of hours considered, the lower the capacity credit for PV. The high fraction of hours and explicit inclusion of winter evenings in the ISO-defined capacity credit calculations for NYISO and ISONE, in conjunction with the relatively low capacity factor of PV in the Northeast, leads to a low capacity credit for these ISOs. As CAISO does not specify specific hours for the PV capacity credit calculation, we only include the capacity factor calculated over peak-net-load hours, which has fallen from a median value of 53% in 2010 to 25% in 2017 as increased PV generation has pushed peak-net-load hours to the morning and evening.

Fig. 3c shows the calculated capacity revenues over time, using the ISO-defined critical hours for MISO, PJM, NYISO, and ISONE and the top 7.04% of net-load hours for CAISO. For most nodes and years the capacity revenue is small compared to the energy revenue (Fig. 2b), but for some nodes—particularly those centered around New York City, and the Boston area in 2017—the capacity revenue can reach 40%–80% of the energy revenue. The PJM and NYISO markets demonstrate the most within-ISO variability in capacity revenues, driven by large variation in capacity prices between their constituent capacity zones: in NYISO the interquartile range (IQR) of capacity revenues is $\geq 25\$/kW_{ac}$ per year in each year, and in both PJM and NYISO the IQR is $\geq 42\$/kW_{ac}$ per year in at least one year.

3.3. PV health and climate benefits

Marginal public health benefits from PV generation arising from SO_2, NO_x, and $PM_{2.5}$ emissions mitigation have been declining with time in MISO, PJM, NYISO, and ISONE (Fig. 4a), as noted by Millstein et al. [10]. In spite of this decline, median public health benefits in 2017 are still substantial, equating to roughly 70% of median 2017 energy revenue in MISO, 100% in PJM, and 70% in NYISO (Fig. 2b). The majority of public health benefits over the time period analyzed have resulted from SO_2 mitigation, as shown in Fig. SI.35, which disaggregates benefits by pollutant. Some of the highest-health-benefit nodes—such as those in New York City—do not necessarily have high marginal emissions rates, but have large associated damages resulting from their high population density.

CO_2 emissions offsets associated with PV generation, shown in Fig. 4b, have been more stable than SO_2, NO_x, and $PM_{2.5}$ offsets over the time period analyzed, suggesting that the decline in air pollutant emissions has primarily resulted from the adoption of tighter air-quality standards and installation of SO_2- and NO_x-control technologies.

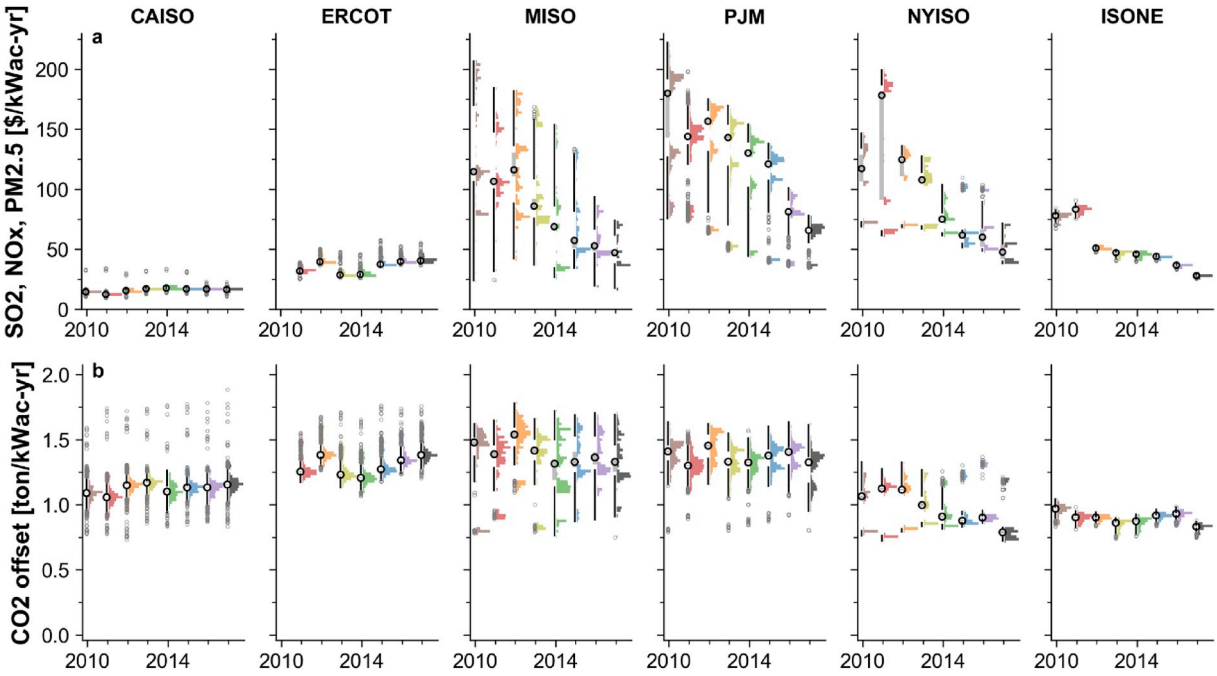

Fig. 4. Public health and climate benefits from PV generation by ISO. a, Distribution of modeled public health benefits associated with SO_2, NO_x, and $PM_{2.5}$ mitigation by 1-axis-tracking PV arrays across nodes within each ISO. Marginal damage rates are calculated using the EASIUR model [46]. **b**, Modeled CO_2 abatement associated with PV generation at nodes within each ISO. Marginal emissions rates are from Azevedo et al. [46]. Marginal damages and emissions rates are differentiated by operational year, eGRID region, season, and hour of day; nodes are assigned to eGRID regions based on their geographic location (Figs. 1 and SI.4).

While *average* CO_2 emissions rates across ISOs have declined as a result of increased natural gas and renewables generation (Fig. SI.5) [109], the distribution of marginal generators has undergone little change [10], leading to a relatively small change in marginal CO_2 emissions rates over time (Fig. SI.6) [46].

4. PV system breakeven costs

To assess the competitiveness of an investment in PV capacity at a given node, we calculate the net present value (NPV) of PV electricity assuming that the value of PV services described above (energy, capacity, and emissions mitigation) for a given year is maintained for the duration of the plant's life, solving for the "breakeven" upfront cost that would set the NPV to zero.

The NPV is given by

$$\mathrm{NPV} = \sum_{t=1}^{L} \frac{((R + C_{\mathrm{CO_2}} M_{\mathrm{CO_2}})(1-d)^t - C_{\mathrm{OM}})(1-T) + \frac{D_t}{(1+i)^t} C_{\mathrm{PV}} T}{(1+\rho)^t} - C_{\mathrm{PV}}(1-\delta) \quad (9)$$

where L is the lifetime of the PV array; R is the yearly PV revenue, including contributions from energy (Fig. 2b), capacity (Fig. 3c), and public health (Fig. 4a) where noted; C_{CO_2} is the price on carbon emissions; M_{CO_2} is the annual marginal CO_2 displaced per unit of PV capacity in a given ISO (Fig. 4b); d is the annual degradation rate in PV output; C_{OM} is the annual operations and maintenance cost; T is the combined federal and state tax rate; D_t is the percentage of the upfront cost depreciated in year t using the 5-year Modified Accelerated Cost Recovery System (MACRS), assuming the PV owner can completely monetize the tax benefits of depreciation; i is the annual inflation rate; ρ is the real weighted average cost of capital (WACC); δ is the federal investment tax credit (ITC); and C_{PV} is the upfront system cost [110]. Numerical values and sources for financial parameters are given in Table 2. The effects of state and local subsidies are not included here, and the ITC is set to $\delta = 0\%$ unless noted otherwise. Calculated breakeven costs are sensitive to input assumptions, particularly regarding the WACC, as shown in Fig. SI.37.

Fig. 5b shows the distribution in calculated breakeven PV cost across all nodes in 2017 considering different collections of PV services, compared to observed upfront PV system costs (Fig. 5a) [1]. Under the stated financial assumptions and considering the value of energy, capacity, and public health benefits (green curves, leaving out climate benefits), PV would break even at the 2017 upfront cost of 1.44 $/ W_{ac} at 30% of the modeled nodes, ranging from 0% of nodes in CAISO, MISO, and ISONE to ~ 50% in NYISO and ~60% in PJM.

Table 2
Default assumptions for net-present-value calculation.

Parameter	Symbol	Value	Units	Reference
PV array lifetime	L	30	[years]	[1]
Revenue (energy, capacity, health)	R	*calculated*	[$/kW$_{ac}$ per year]	
CO_2 price	C_{CO_2}	[0, 50, 100]	[$/ton$CO_2$]	
CO_2 displacement	M_{CO_2}	*calculated*	[ton/kW$_{ac}$ per year]	
Degradation rate	d	−0.5	[%/year]	[111, 112]
Operations & maintenance cost	C_{OM}	20	[$/kW$_{ac}$ per year]	[1]
Federal & state tax rate	T	28	[%]	[113]
5-year MACRS depreciation in year t	D_t	*variable*	[%]	[114]
Inflation rate	i	2.5	[%]	[1]
Real weighted average cost of capital	ρ	7.0	[%]	[115]
Investment tax credit	δ	0	[%]	

At a carbon price of 50 $/ton$CO_2$ (corresponding to the central value for 2020 historically used by the U.S. federal government [117]), PV would break even at ~75% of the modeled nodes, ranging from 5% in CAISO to 100% in ERCOT, MISO, and PJM. A small reduction in upfront PV cost would deliver large gains: with a 10% reduction in PV upfront cost, PV would break even at 90% of modeled nodes and 50% of CAISO nodes.

At a carbon price of 100 $/ton$CO_2$, which approaches the floor price estimated to be necessary to achieve the goals of the 2015 Paris agreement (floor price estimates in the literature range from 116 $/ton$CO_2$ to at least 220 $/ton$CO_2$ [118–122]), PV at today's upfront cost would break even at 100% of nodes in all ISOs. A recent macroeconomic study reports a global social cost of carbon of 417 $/ton$CO_2$ [123]; at this carbon price, PV would break even at all nodes in all years on the basis of climate benefits alone at a PV system cost of 3 $/W$_{ac}$.

If only market revenues from energy and capacity are counted (neglecting social benefits from abated emissions), median breakeven costs in 2017 range from 0.50 $/W$_{ac}$ in MISO to 0.85 $/W$_{ac}$ in NYISO. An alternative metric is the breakeven carbon price: as shown in Fig. 5c, at the 2017 upfront PV cost of 1.44 $/W$_{ac}$, median breakeven carbon prices range from 0 $/ton$CO_2$ in PJM to 60 $/ton$CO_2$ in CAISO in 2017 if energy, capacity, and public health values are included, and from 45 $/ton$CO_2$ in PJM to 80 $/ton$CO_2$ in ISONE if only energy and capacity are included.

As noted above, energy and capacity revenues and the value of abated emissions demonstrate a large amount of variability from year to year, so the breakeven costs for 2017 shown in Fig. 5b and c do not hold for all years. Some of the drivers of this variability—such as variations in gas price, hydropower availability, and capacity price—are relatively cyclical, while others—such as the decline in PV value factor and capacity credit in CAISO and the decline in marginal health benefits associated with the adoption of emissions-control measures—reflect longer-term trends that appear unlikely to change direction. To illustrate the effect of year-to-year price variations, Fig. 5d shows the calculated breakeven PV costs using different yearly profiles for energy and capacity prices, including a 50 $/ton CO_2 price but leaving out marginal health benefits (which, as noted above, appear unlikely to return to the high levels witnessed early in the decade). Breakeven costs for 2017 are near the bottom of the distribution over the years analyzed, as natural gas prices (and correspondingly LMPs) in 2017 were at the low end of their distribution over 2010–2017 [132]. Averaging the calculated energy, capacity, and climate benefits over 2010–2017 (heavy black lines in Fig. 5d), PV breaks even at 2017 PV costs at ~85% of modeled nodes, from ≤25% in MISO and ISONE to ~55% in NYISO, 80% in CAISO, and ≥ 98% in ERCOT and PJM.

The discussion above addresses PV generators in a hypothetical policy environment where health and climate impacts are internalized. Fig. 6 shows PV system breakeven costs averaged over 2010–2017 under alternative economic assumptions. Starting from a baseline including energy and capacity market revenues alone, Fig. 6 compares the impacts of reducing financing costs (here demonstrated by lowering the WACC from the default assumption of 7% [115] to 4%, reflecting values used by the EPA [125] and reported by other sources [126–128]); including the 30% ITC, which at the time of this writing applies to systems built before 2020 [124]; monetizing health benefits at 2017 levels (Fig. 4); and applying different levels of carbon pricing. The relative impact of these different assumptions varies by ISO: in lower-emissions systems such as CAISO, NYISO, and ISONE the 30% ITC has a larger impact on PV profitability than the individual contributions of public health benefits or a 50 $/ton CO_2 price, while in MISO the individual contributions of public health benefits and carbon pricing are both larger than the ITC. At a PV system cost of 1.44 $/W$_{ac}$, PV breaks even at 1% of modeled nodes across the U.S. on the basis of energy and capacity revenues with default financial assumptions; at 33% of nodes with a reduction in the WACC from 7% to 4%; at 51% of nodes with health benefits monetized at 2017 levels; at 64% of nodes with the 30% ITC; at 83% of nodes with a

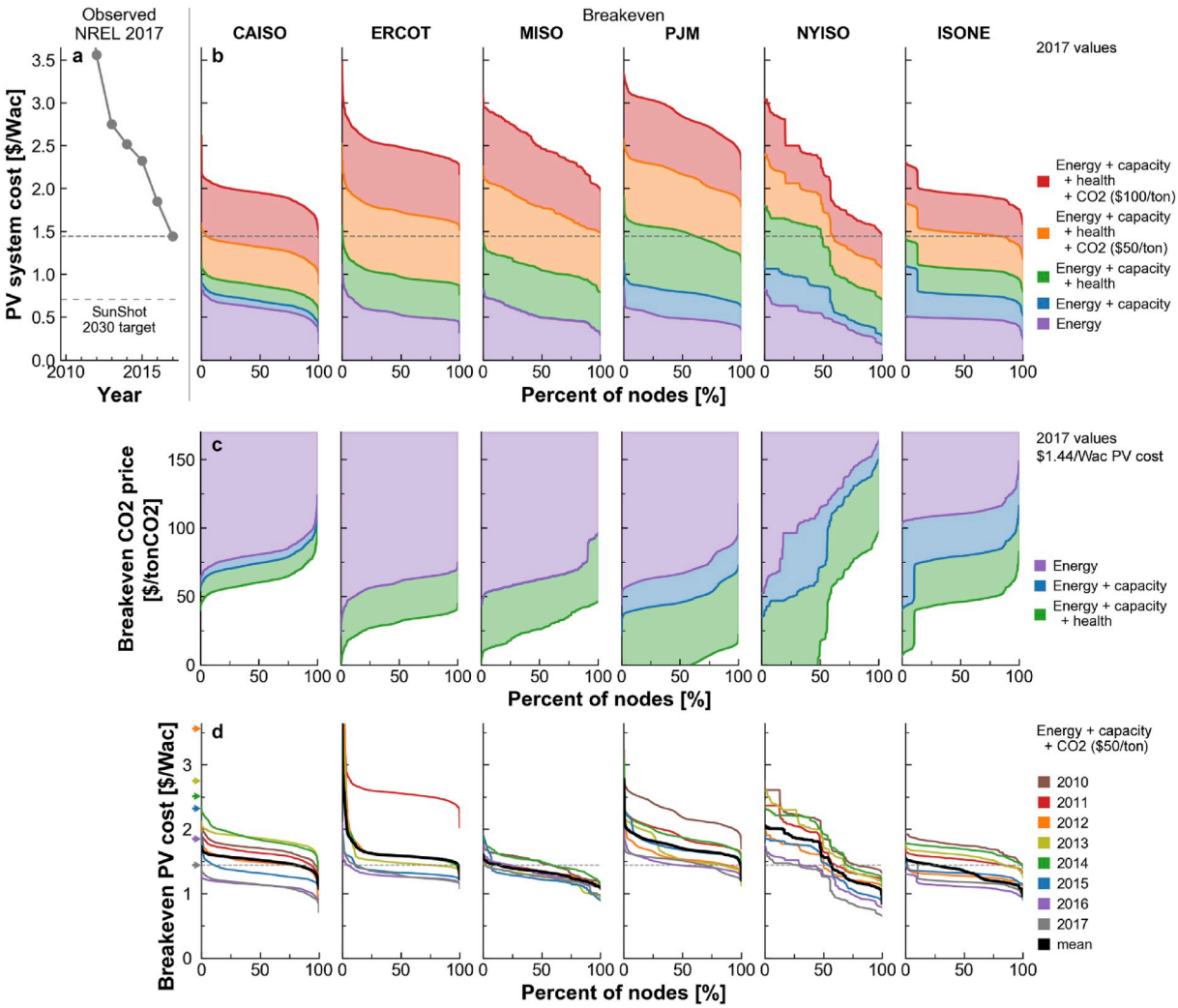

Fig. 5. Observed capital cost and distribution of breakeven costs for PV arrays across all modeled nodes. Observed PV capital costs (**a**) are taken from Fu et al. [1] for a 100 MW 1-axis-tracking PV array. The U.S. Department of Energy SunShot PV cost target for 2030 is included in **a** for context [116]. Each trace in **b** shows the percentage of nodes across each ISO that would break even below the corresponding upfront system cost on the y-axis, assuming that the nodal revenue in 2017 persists for the lifetime of the system. Colored traces and areas indicate the cumulative inclusion of revenue from the wholesale energy (LMP) market (purple), capacity market (blue), public health benefits (green), carbon mitigation assuming a 50 $/ton CO_2 price (orange), and carbon mitigation assuming an additional 50 $/ton CO_2 price (100 $/ton total) (red). Dotted lines are included at 1.44 $\$/W_{ac}$, the 2017 observed PV system cost, to guide the eye. **c**, Breakeven CO_2 prices for PV in 2017, assuming an upfront system cost of 1.44 $\$/W_{ac}$. Note that in **c**, PV breaks even at CO_2 prices above the plotted line; in plots of the breakeven PV system cost (**b**,**d**), PV breaks even at upfront costs below the plotted line. **d**, Breakeven upfront costs for energy, capacity, and climate benefits for 2010–2017 profile years, assuming a 50 $/ton CO_2 price. In **d**, colored arrows along the leftmost y-axis indicate the observed upfront PV system costs for each year shown in **a**. The black trace labeled "mean" is the nodal average breakeven cost, including all available years of data for each node. Fig. SI.38 in the Supplementary Information shows yearly breakeven costs under alternative carbon price assumptions. (For interpretation of the references to color in this figure legend, the reader is referred to the Web version of this article.)

50 $/ton CO_2 price; and at $\geq$ 99.9% of nodes with a 100 $/ton CO_2 price. It is notable that under 2010–2017 electricity prices and representative 2017 policy conditions (namely, including the 30% ITC but without a substantial price on CO_2 or air pollutant emissions), utility-scale PV breaks even at nearly two-thirds of modeled nodes.

5. Conclusions

While the marginal value and upfront system cost of PV have both declined over the last decade, the results described here suggest that cost decline has outpaced value decline, such that in 2017 the net benefits of utility-scale PV outweigh the cost across the majority of U.S. electricity markets when the social benefits of particulate matter and CO_2 emissions abatement are included. Current cap-and-trade market prices for CO_2 and SO_2 emissions are much lower than estimates of the social cost of emissions, suggesting that emissions caps should be lowered (or that emissions floor prices should be raised) in order to provide appropriate incentives for low-carbon generation sources such as PV. A next-best alternative to instituting appropriate emissions prices is to tailor PV deployment support mechanisms to reflect spatial differences in the benefits of PV generation. Persistent transmission congestion over the time period analyzed results in variation in the energy, capacity, health, and climate benefits of a unit of PV generation capacity depending on its location of interconnection with the electric grid. As shown in Fig. 4a, nodal public health benefits from PV generation in the New York ISO have varied by roughly a factor of 2 across the state in any given year from 2010 to 2017, but existing renewable energy credits reward generation equally, irrespective of its location within the state.

The analysis described here applies primarily to utility-scale generators on the transmission grid, which are exposed to the spatially- and

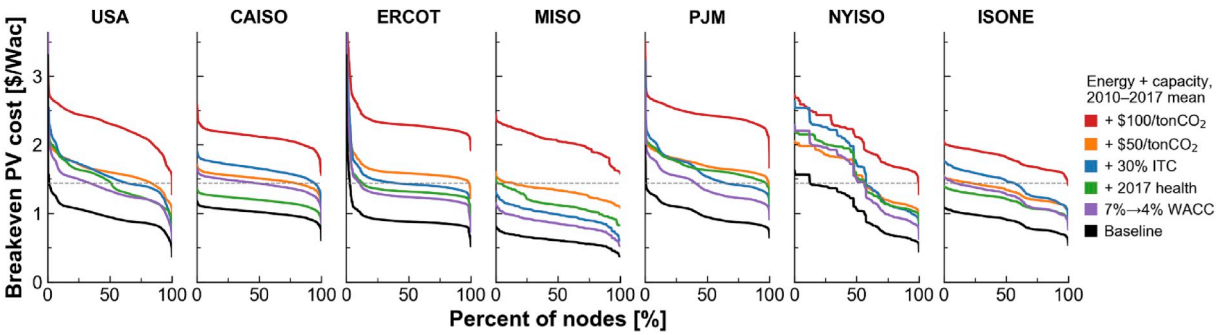

Fig. 6. Distribution of breakeven costs for PV arrays across all modeled nodes under alternative economic assumptions. Each trace shows the percentage of nodes across each ISO (or, for the leftmost subplot labeled "USA", across all ISOs and nodes) that would break even below the corresponding upfront system cost on the y-axis, assuming that the nodal revenue in the modeled years persists for the lifetime of the system. Breakeven upfront costs are averaged over 2010–2017 based on energy and capacity revenues under the default assumptions listed in Table 2 (black trace) and under alternative assumptions: decreasing the WACC from $\rho = 7\%$ to 4% (purple trace); including nodal public health benefits from SO_2, NO_x, and $PM_{2.5}$ mitigation at 2017 levels from Fig. 4a (green trace); setting the investment tax credit to its 2019 value of $\delta = 30\%$ (blue trace) [124]; including climate benefits averaged over 2010–2017 valued at 50 \$/ton CO_2 (orange trace, showing the same results as the black "mean" trace in Fig. 5d); and including climate benefits averaged over 2010–2017 valued at 100 \$/ton CO_2 (red trace). Alternative assumptions are applied individually to the baseline case and are not cumulative. Dotted lines are included at 1.44 $\$/W_{ac}$, the 2017 observed PV system cost [1], to guide the eye. Fig. SI.38 in the Supplementary Information shows individual yearly breakeven costs for each assumption. (For interpretation of the references to color in this figure legend, the reader is referred to the Web version of this article.)

temporally-varying signals provided by the LMP. Residential and small commercial electricity customers on the distribution grid typically are not exposed to such signals, leading to installation incentives that are not necessarily matched to the system value of PV energy. Passing the spatial and temporal signals from the LMP (along with appropriate emissions prices) as far into the distribution system as possible could help steer PV deployment to congested high-price locations, reducing prices for other electricity consumers and ensuring that distributed and utility-scale solar generators can compete on equal footing [129].

It is important to emphasize that the breakeven costs shown here are for a marginal unit of PV capacity. As grid conditions change—through continued deployment of renewables, expansion of transmission capacity, retirement of existing plants, shifts in the price of natural gas, variations in hydropower availability, changes in climate and demand patterns, and evolution in other factors—there will be associated changes in LMP, net load, and marginal emissions rate profiles, leading to corresponding changes in the breakeven cost for PV and other technologies. Current electricity market designs, particularly regarding resource adequacy, will also need to be adjusted to adapt to generation mixes dominated by low- and zero-marginal-cost sources [130,131]. On the whole, the upfront cost whereat PV breaks even is expected to decline with increasing PV penetration [6], necessitating continued cost reductions for PV. Nevertheless, the experience so far in CAISO, where despite its 5–10× higher PV penetration than the other ISOs, PV would still break even at most nodes at an upfront cost within 10% of observed 2017 costs, suggests that there is still considerable room for competitive PV expansion across the continental U.S., particularly in the interior and mid-Atlantic regions. The strategies presented here for assessing the locational value of PV electricity can be extended to other distributed energy resources such as wind power [16] and energy storage [110], and incorporation of spatial, temporal, and technological resolution will become increasingly important as the electric power system evolves and relies increasingly on variable renewable energy resources.

Data and computer code availability

Python scripts for data acquisition, data cleaning, modeling, validation, analysis, and visualization, along with nodal LMPs and numerical results described above, are available at https://doi.org/10.5281/zenodo.3562896.DJ3O6myVLVh5Qa.

Author contributions

P.R.B. and F.M.O'S. conceived of the study. P.R.B. collected all data, performed all calculations and analysis, and wrote the paper. F.M.O'S. provided comments on the manuscript.

Declaration of interests

Both authors are affiliated with the MIT Energy Initiative, which receives funding from a variety of external sources including utility companies, oil and gas producers, renewable energy companies, private philanthropic organizations, and environmental non-profits, listed at http://energy.mit.edu/membership/#current-members. None of these organizations were involved with the development of the work reported here. F.M.O'S. is Senior Vice President of Lincoln Clean Energy, LLC, a developer and owner of wind and solar projects in the United States.

Acknowledgments

P.R.B. and the work reported here are supported by the U.S. Department of Energy (DOE) Office of Energy Efficiency and Renewable Energy (EERE) Postdoctoral Research Award through the EERE Solar Energy Technologies Office (SETO) under DOE contract number DE-SC00014664. P.R.B. acknowledges A. Botterud, J. Jean, J. Jenkins, S. Burger, S. Kurtz, R. van Haaren, D. Weiss, E. Dimantchev, and E. Gençer for insightful discussions, A. Brocks for assistance with capacity market data, and J. Jenkins and S. Burger for assistance with node locations. P. R.B. also acknowledges the administrators and staff of the MIT Supercloud and the authors of the open-source software packages and public data sources used in this analysis, and representatives from ERCOT and ISONE for access to data not available publicly. All views expressed in this paper are those of the authors and do not necessarily reflect the views of DOE, EERE, SETO, or acknowledged individuals.

Appendix A. Supplementary data

Supplementary data to this article can be found online at https://doi.org/10.1016/j.rser.2019.109594.

References

[1] Fu R, Chung D, Lowder T, Feldman D, Ardani K. U.S. Solar photovoltaic system cost benchmark: Q1 2017. Report. National Renewable Energy Laboratory; 2017. https://doi.org/10.2172/1390776.

[2] REN21. Renewables 2018 global status report. Report. Renewable Energy Poicy Network for the 21st Century; 2018. https://www.ren21.net/wp-content/uploads/2019/08/Full-Report-2018.pdf.

[3] Sensfuß F, Ragwitz M, Genoese M. The merit-order effect: a detailed analysis of the price effect of renewable electricity generation on spot market prices in Germany. Energy Policy 2008;36:3076–84. https://doi.org/10.1016/j.enpol.2008.03.035.

[4] Lamont AD. Assessing the long-term system value of intermittent electric generation technologies. Energy Econ 2008;30:1208–31. https://doi.org/10.1016/j.eneco.2007.02.007.

[5] Woo CK, Moore J, Schneiderman B, Ho T, Olson A, Alagappan L, Chawla K, Toyama N, Zarnikau J. Merit-order effects of renewable energy and price divergence in California's day-ahead and real-time electricity markets. Energy Policy 2016;92:299–312. https://doi.org/10.1016/j.enpol.2016.02.023.

[6] Wiser R, Mills A, Seel J, Levin T, Botterud A. Impacts of variable renewable energy on bulk power system Assets, pricing, and costs. Report. Lawrence Berkeley National Laboratory and Argonne National Laboratory; 2017. https://emp.lbl.gov/publications/impacts-variable-renewable-energy.

[7] Mills A, Wiser R. Changes in the economic value of variable generation at high penetration levels: a pilot case study of California. Report. Lawrence Berkeley National Laboratory; 2012. http://emp.lbl.gov/sites/all/files/lbnl-5445e.pdf.

[8] Hirth L. The market value of variable renewables. The effect of solar wind power variability on their relative price. Energy Econ 2013;38:218–36. https://doi.org/10.1016/j.eneco.2013.02.004.

[9] Mills AD, Wiser RH. Changes in the economic value of photovoltaic generation at high penetration levels: a pilot case study of California. IEEE J Photovolt 2013;3:1394–402. https://doi.org/10.1109/JPHOTOV.2013.2263984.

[10] Millstein D, Wiser R, Bolinger M, Barbose G. The climate and air-quality benefits of wind and solar power in the United States. Nature Energy 2017;2:17134. https://doi.org/10.1038/nenergy.2017.134.

[11] Mills AD, Wiser RH. Strategies to mitigate declines in the economic value of wind and solar at high penetration in California. Appl Energy 2015;147:269–78. https://doi.org/10.1016/j.apenergy.2015.03.014.

[12] Braff WA, Mueller JM, Trancik JE. Value of storage technologies for wind and solar energy. Nat Clim Chang 2016;6:964–9. https://doi.org/10.1038/nclimate3045.

[13] Hirth L, Müller S. System-friendly wind power. How advanced wind turbine design can increase the economic value of electricity generated through wind power. Energy Econ 2016;56:51–63. https://doi.org/10.1016/j.eneco.2016.02.016.

[14] Johansson V, Thorson L, Goop J, Göransson L, Odenberger M, Reichenberg L, Taljegard M, Johnsson F. Value of wind power – implications from specific power. Energy 2017;126:352–60. https://doi.org/10.1016/j.energy.2017.03.038.

[15] Callaway D, Fowlie M, McCormick G. Location, location, location: the variable value of renewable energy and demand-side efficiency resources. Journal of the Association of Environmental and Resource Economists 2018;5:39–75. https://doi.org/10.1086/694179.

[16] Mills AD, Millstein D, Jeong S, Lavin L, Wiser R, Bolinger M. Estimating the value of offshore wind along the United States' Eastern Coast. Environ Res Lett 2018;13:094013. https://doi.org/10.1088/1748-9326/aada62.

[17] Siler-Evans K, Lima I, Morgan MG, Apt J. Regional variations in the health, environmental, and climate benefits of wind and solar generation. Proc Natl Acad Sci 2013;110:11768–73. https://doi.org/10.1073/pnas.1221978110.

[18] Buonocore JJ, Luckow P, Norris G, Spengler JD, Biewald B, Fisher J, Levy JI. Health and climate benefits of different energy-efficiency and renewable energy choices. Nat Clim Chang 2016;6:100–6. https://doi.org/10.1038/nclimate2771.

[19] Vaishnav P, Horner N, Azevedo IL. Was it worthwhile? Where have the benefits of rooftop solar photovoltaic generation exceeded the cost? Environ Res Lett 2017;12:094015. https://doi.org/10.1088/1748-9326/aa815e.

[20] Branker K, Pathak M, Pearce J. A review of solar photovoltaic levelized cost of electricity. Renew Sustain Energy Rev 2011;15:4470–82. https://doi.org/10.1016/j.rser.2011.07.104.

[21] Rhodes JD, King C, Gulen G, Olmstead SM, Dyer JS, Hebner RE, Beach FC, Edgar TF, Webber ME. A geographically resolved method to estimate levelized power plant costs with environmental externalities. Energy Policy 2017;102:491–9. https://doi.org/10.1016/j.enpol.2016.12.025.

[22] US Energy Information Administration. Levelized cost and levelized avoided cost of new generation resources in the Annual Energy Outlook 2019. 2019. https://www.eia.gov/outlooks/aeo/pdf/electricity_generation.pdf.

[23] Ryan L, Dillon J, Monaca SL, Byrne J, O'Malley M. Assessing the system and investor value of utility-scale solar PV. Renew Sustain Energy Rev 2016;64:506–17. https://doi.org/10.1016/j.rser.2016.06.004.

[24] Borenstein S. The market value and cost of solar photovoltaic electricity production. Report. University of California Energy Institute; 2008. https://escholarship.org/uc/item/3ws6r3j4.

[25] Hansen L, Lacy V, Glick D. A review of solar PV benefit & cost studies. Report. Rocky Mountain Institute; 2013. https://rmi.org/wp-content/uploads/2017/05/RMI_Document_Repository_Public-Reprts_eLab-DER-Benefit-Cost-Deck_2nd_Edition131015.pdf.

[26] California ISO (CAISO). Market price maps. http://www.caiso.com/PriceMap/Pages/default.aspx; 2018.

[27] Midwest ISO (MISO). LMP contour map. https://api.misoenergy.org/MISORTWD/lmpcontourmap.html; 2018.

[28] PJM Interconnection. Markets & operations - data directory. https://www.pjm.com/markets-and-operations/data-dictionary.aspx; 2014.

[29] New York ISO (NYISO). Comprehensive system planning process (CSPP). https://www.nyiso.com/cspp; 2018.

[30] California ISO (CAISO). California ISO oasis. http://oasis.caiso.com/mrioasis/logon.do; 2018.

[31] Electric Reliability Council of Texas (ERCOT). Market prices. http://www.ercot.com/mktinfo/prices; 2018.

[32] Midwest ISO (MISO). Market reports. https://www.misoenergy.org/markets-and-operations/real-time–market-data/market-reports/; 2018.

[33] Midwest ISO (MISO). Market report archives. https://www.misoenergy.org/markets-and-operations/real-time–market-data/market-reports/market-report-archives/; 2018.

[34] PJM Interconnection. Daily day-ahead LMP. http://www.pjm.com/markets-and-operations/energy/day-ahead/lmpda.aspx; 2018.

[35] New York ISO (NYISO). Pricing data. http://mis.nyiso.com/public/; 2018.

[36] ISO New England (ISONE). Hourly day-ahead LMPs. https://www.iso-ne.com/isoexpress/web/reports/pricing/-/tree/lmps-da-hourly; 2018.

[37] U.S. Energy Information Administration. Form EIA-860 detailed data. https://www.eia.gov/electricity/data/eia860/; 2018.

[38] National Renewable Energy Laboratory. The OpenPV project. https://openpv.nrel.gov/; 2018.

[39] Habte A, Sengupta M, Lopez A. Evaluation of the national solar radiation database (NSRDB): 1998-2015. Report. National Renewable Energy Laboratory; 2017. http://www.nrel.gov/docs/fy17osti/67722.pdf.

[40] Sengupta M, Xie Y, Lopez A, Habte A, Maclaurin G, Shelby J. The national solar radiation data base (NSRDB). Renew Sustain Energy Rev 2018;89:51–60. https://doi.org/10.1016/j.rser.2018.03.003.

[41] Holmgren WF, Hansen CW, Mikofski MA. PVLIB Python: a Python package for modeling solar energy systems. Journal of Open Source Software 2018;3:884. https://doi.org/10.21105/joss.00884.

[42] PV Performance Modeling Collaborative. PVLIB toolbox. 2018. https://pvpmc.sandia.gov/applications/pv_lib-toolbox/.

[43] Brown PR, O'Sullivan FM. Shaping photovoltaic array output to align with changing wholesale electricity price profiles. Appl Energy 2019;256:113734. https://doi.org/10.1016/j.apenergy.2019.113734.

[44] U.S. Energy Information Administration. Form EIA-923 detailed data. https://www.eia.gov/electricity/data/eia923/; 2018.

[45] National Renewable Energy Laboratory. PVDAQ (PV data acquisition). https://developer.nrel.gov/docs/solar/pvdaq-v3/; 2018.

[46] Azevedo IL, Horner NC, Siler-Evans K, Vaishnav PT. Electricity marginal factors estimates. Report, center for climate and energy decision making. Pittsburgh: Carnegie Mellon University; 2017. https://cedm.shinyapps.io/MarginalFactors/.

[47] U.S. Environmental Protection Agency (EPA). Emissions and generation resource integrated database (eGRID). https://www.epa.gov/energy/emissions-generation-resource-integrated-database-egrid; 2018.

[48] Siler-Evans K, Azevedo IL, Morgan MG. Marginal emissions factors for the U.S. electricity system. Environ Sci Technol 2012;46:4742–8. https://doi.org/10.1021/es300145v.

[49] Center for Climate and Energy Decision Making. EASIUR: marginal social costs of emissions in the United States. https://barney.ce.cmu.edu/~jinhyok/easiur/; 2015.

[50] Heo J, Adams PJ, Gao HO. Public health costs of primary PM2.5 and inorganic PM2.5 precursor emissions in the United States. Environ Sci Technol 2016;50:6061–70. https://doi.org/10.1021/acs.est.5b06125.

[51] Heo J, Adams PJ, Gao HO. Reduced-form modeling of public health impacts of inorganic PM2.5 and precursor emissions. Atmos Environ 2016;137:80–9. https://doi.org/10.1016/j.atmosenv.2016.04.026.

[52] U.S. Department of Labor - Bureau of Labor Statistics. Consumer price Index. https://data.bls.gov/timeseries/CUUR0000SA0; 2018.

[53] California Public Utilities Commission. Resource adequacy. https://www.cpuc.ca.gov/RA/; 2019.

[54] Midwest ISO (MISO). Resource adequacy. 2019. https://www.misoenergy.org/planning/resource-adequacy/#nt=%2Fplanningdoctype%3APRA_Document&t=10&p=0&s=&sd=.

[55] PJM Interconnection. Capacity market (RPM). https://www.pjm.com/markets-and-operations/rpm.aspx; 2019.

[56] New York ISO (NYISO). Strip auction summary. 2019. http://icap.nyiso.com/ucap/public/auc_view_strip_detail.do.

[57] ISO New England (ISONE). Forward capacity auction results. https://www.iso-ne.com/isoexpress/web/reports/auctions/-/tree/fca-results; 2018.

[58] New York ISO (NYISO). NYISO pricing information. 2019. http://www.nyiso.com/public/site/js/maps.js.

[59] PJM Interconnection. Pricing nodes. 2019. https://dataminer2.pjm.com/feed/pnode/definition.

[60] U.S. Federal Energy Regulatory Commission. Form No. 714 - annual electric balancing authority area and planning area report. https://www.ferc.gov/docs-filing/forms/form-714/data.asp; 2018.

[61] Muller BNZ, Mendelsohn R, Nordhaus W. Environmental accounting for pollution in the United States economy. Am Econ Rev 2011;101:1649–75. https://doi.org/10.1257/aer.101.5.1649.

[62] Muller NZ. Boosting GDP growth by accounting for the environment. Science 2014;345:873–4. https://doi.org/10.1126/science.1253506.

[63] Muller NZ. AP3 (AP2, APEEP) model. https://public.tepper.cmu.edu/nmuller/APModel.aspx; 2018.
[64] Stein JS, Holmgren WF, Forbess J, Hansen CW. PVLIB: open source photovoltaic performance modeling functions for Matlab and Python. Proceedings of the IEEE Photovoltaic Specialist Conference 2016;43:3425–30. https://doi.org/10.1109/PVSC.2016.7750303.
[65] Dobos AP. PVWatts version 5 manual. Report. National Renewable Energy Laboratory; 2014. https://www.nrel.gov/docs/fy14osti/62641.pdf.
[66] National Renewable Energy Laboratory. PVWatts calculator - version 5. 2018. https://pvwatts.nrel.gov/version_5.php.
[67] Bolinger M, Seel J, Lacommare KH. Utility-scale solar 2016: an empirical analysis of project cost, performance, and pricing trends in the United States. Report. Lawrence Berkeley National Laboratory; 2017. https://emp.lbl.gov/publications/utility-scale-solar-2016-empirical.
[68] Lorenzo E, Narvarte L, Muñoz J. Tracking and back-tracking. Prog Photovolt Res Appl 2011;19:747–53. https://doi.org/10.1002/pip.1085.
[69] Reindl D, Beckman W, Due J. Diffuse fraction correlations. Sol Energy 1990;45:1–7. https://doi.org/10.1016/0038-092X(90)90060-P.
[70] Loutzenhiser PG, Manz H, Felsmann C, Strachan PA, Frank T, Maxwell GM. Empirical validation of models to compute solar irradiance on inclined surfaces for building energy simulation. Sol Energy 2007;81:254–67. https://doi.org/10.1016/j.solener.2006.03.009.
[71] Reda I, Andreas A. Solar position algorithm for solar radiation applications. Sol Energy 2004;76:577–89. https://doi.org/10.1016/j.solener.2003.12.003.
[72] Reda I, Andreas A. Solar position algorithm for solar radiation applications (revised). Report. National Renewable Energy Laboratory; 2008. https://www.nrel.gov/docs/fy08osti/34302.pdf.
[73] King DL, Boyson WE, Kratochvil JA. Photovoltaic array performance model. Report. Sandia National Laboratories; 2004. https://doi.org/10.2172/919131.
[74] Garver LL. Effective load carrying capability of generating units. IEEE Transactions on Power Apparatus and Systems *PAS* 1966;85:910–9. https://doi.org/10.1109/TPAS.1966.291652.
[75] Pelland S, Abboud I. Comparing photovoltaic capacity value metrics: a case study for the city of Toronto. Prog Photovolt Res Appl 2008;16:715–24. https://doi.org/10.1002/pip.864.
[76] Keane A, Milligan M, Dent CJ, Hasche B, D'Annunzio C, Dragoon K, Holttinen H, Samaan N, Söder L, O'Malley M. Capacity value of wind power. IEEE Trans Power Syst 2011;26:564–72. https://doi.org/10.1109/TPWRS.2010.2062543.
[77] Madaeni SH, Sioshansi R, Denholm P. Comparison of capacity value methods for photovoltaics in the western United States. Report July. National Renewable Energy Laboratory; 2012. https://doi.org/10.2172/1046871.
[78] Madaeni SH, Sioshansi R, Denholm P. Comparing capacity value estimation techniques for photovoltaic solar power. IEEE J Photovolt 2013;3:407–15. https://doi.org/10.1109/JPHOTOV.2012.2217114.
[79] Dent CJ, Sioshansi R, Reinhart J, Wilson AL, Zachary S, Lynch M, Bothwell C, Steele C. Capacity value of solar power: report of the IEEE PES task force on capacity value of solar power. In: 2016 international conference on probabilistic methods applied to power systems (PMAPS). IEEE, Beijing); 2016. p. 1–7. https://doi.org/10.1109/PMAPS.2016.7764197.
[80] Bothwell C, Hobbs BF. Crediting wind and solar renewables in electricity capacity markets: the effects of alternative definitions upon market efficiency. Energy J 2017;38:173–88. https://doi.org/10.5547/01956574.38.SI1.cbot.
[81] Byers C, Levin T, Botterud A. Capacity market design and renewable energy: performance incentives, qualifying capacity, and demand curves. Electr J 2018;31:65–74. https://doi.org/10.1016/j.tej.2018.01.006.
[82] Madaeni SH, Sioshansi R, Denholm P. Estimating the capacity value of concentrating solar power plants: a case study of the Southwestern United States. IEEE Trans Power Syst 2012;27:1116–24. https://doi.org/10.1109/TPWRS.2011.2179071.
[83] California ISO (CAISO). Renewables and emissions reports. 2018. http://www.caiso.com/market/Pages/ReportsBulletins/RenewablesReporting.aspx.
[84] Electric Reliability Council of Texas (ERCOT). Hourly aggregated wind output. 2018. http://www.ercot.com/gridinfo/generation.
[85] PJM Interconnection. Wind generation. 2018. https://dataminer2.pjm.com/feed/wind_gen/definition.
[86] ISO New England (ISONE). Daily generation by fuel type. https://www.iso-ne.com/isoexpress/web/reports/operations/-/tree/daily-gen-fuel-type; 2018.
[87] Midwest ISO (MISO). Business practices manual No. 11 - resource adequacy. Report. Midwest Independent System Operator (MISO); 2018. https://www.misoenergy.org/legal/business-practice-manuals/.
[88] PJM Interconnection. Manual 21: rules and procedures for determination of generating capability. Report. PJM Interconnection; 2017. https://www.pjm.com/library/manuals.aspx.
[89] New York ISO (NYISO). Manual 4 - installed capacity manual. Report. New York: Independent System Operator (NYISO); 2018. https://www.nyiso.com/manuals-tech-bulletins-user-guides.
[90] ISO New England (ISONE). Market rule 1,Section 13 - forward capacity market. Report. ISO New England (ISONE); 2019. https://www.iso-ne.com/participate/rules-procedures/tariff/market-rule-1.
[91] Gami D, Sioshansi R, Denholm P. Data challenges in estimating the capacity value of solar photovoltaics. IEEE J Photovolt 2017;7:1065–73. https://doi.org/10.1109/JPHOTOV.2017.2695328.
[92] Borenstein S. The private and public economics of renewable electricity generation. J Econ Perspect 2012;26:67–92. https://doi.org/10.1257/jep.26.1.67.
[93] Denholm P, Margolis R, Palmintier B, Barrows C, Ibanez E, Bird L. Methods for analyzing the benefits and costs of distributed photovoltaic generation to the U.S. Electric utility system. Report September. National Renewable Energy Laboratory; 2014. http://www.nrel.gov/docs/fy14osti/62447.pdf.
[94] MIT Energy Initiative. The future of solar energy. Report. Cambridge, MA: Massachusetts Institute of Technology; 2015. mitei.mit.edu/futureofsolar.
[95] Cohen MA, Callaway DS. Effects of distributed PV generation on California's distribution system, Part 1: engineering simulations. Sol Energy 2016;128:126–38. https://doi.org/10.1016/j.solener.2016.01.002.
[96] Cohen MA, Kauzmann PA, Callaway DS. Effects of distributed PV generation on California's distribution system, part 2: economic analysis. Sol Energy 2016;128:139–52. https://doi.org/10.1016/j.solener.2016.01.004.
[97] Baker E, Fowlie M, Lemoine D, Reynolds SS. The economics of solar electricity. Annual Review of Resource Economics 2013;5:387–426. https://doi.org/10.1146/annurev-resource-091912-151843.
[98] Clò S, Cataldi A, Zoppoli P. The merit-order effect in the Italian power market: the impact of solar and wind generation on national wholesale electricity prices. Energy Policy 2015;77:79–88. https://doi.org/10.1016/j.enpol.2014.11.038.
[99] Bushnell J, Novan K. Setting with the sun: the impacts of renewable energy on wholesale power markets. 2018. https://ei.haas.berkeley.edu/research/papers/WP292.pdf.
[100] Craig MT, Jaramillo P, Hodge BM, Williams NJ, Severnini E. A retrospective analysis of the market price response to distributed photovoltaic generation in California. Energy Policy 2018;121:394–403. https://doi.org/10.1016/j.enpol.2018.05.061.
[101] Hertwich EG, Gibon T, Bouman EA, Arvesen A, Suh S, Heath GA, Bergesen JD, Ramirez A, Vega MI, Shi L. Integrated life-cycle assessment of electricity-supply scenarios confirms global environmental benefit of low-carbon technologies. Proc Natl Acad Sci USA 2015;112:6277–82. https://doi.org/10.1073/pnas.1312753111.
[102] Hertwich EG, de Larderel JA, Suh S. Green Energy Choices: the benefits, risks and trade-offs of low-carbon technologies for electricity production. Report. United Nations Environment Program; 2016. https://www.resourcepanel.org/reports/green-energy-choices-benefits-risks-and-trade-offs-low-carbon-technologies-electricity.
[103] Lontzek TS, Cai Y, Judd KL, Lenton TM. Stochastic integrated assessment of climate tipping points indicates the need for strict climate policy. Nat Clim Chang 2015;5:441–4. https://doi.org/10.1038/nclimate2570.
[104] Ackerman F, Heinzerling L. Pricing the priceless: cost-benefit analysis of environmental protection, vol. 150. University of Pennsylvania Law Review; 2002. p. 1553. https://doi.org/10.2307/3312947.
[105] Morgan MG, Vaishnav P, Dowlatabadi H, Azevedo IL. Rethinking the social cost of carbon dioxide, vol. 33. Issues in Science and Technology; 2017. https://issues.org/rethinking-the-social-cost-of-carbon-dioxide/.
[106] California Air Resources Board. Archived auction information and results. 2018. https://ww3.arb.ca.gov/cc/capandtrade/auction/auction_notices_and_reports.htm.
[107] Regional Greenhouse Gas Initiative. Allowance prices and volumes. https://www.rggi.org/Auctions/Auction-Results/Prices-Volumes; 2018.
[108] U.S. Environmental Protection Agency (EPA). SO2 Allowance Auctions. https://www.epa.gov/airmarkets/so2-allowance-auctions; 2018.
[109] Schivley G, Azevedo I, Samaras C. Assessing the evolution of power sector carbon intensity in the United States. Environ Res Lett 2018;13. https://doi.org/10.1088/1748-9326/aabe9d.
[110] Salles MBC, Huang J, Aziz MJ, Hogan WW. Potential arbitrage revenue of energy storage systems in PJM. Energies 2017;10:1100. https://doi.org/10.3390/en10081100.
[111] Jordan DC, Kurtz SR. Photovoltaic degradation rates – an analytical review. Prog Photovolt Res Appl 2013;21:12–29. https://doi.org/10.1002/pip.1182.
[112] Jordan DC, Kurtz SR, Vansant K, Newmiller J. Compendium of photovoltaic degradation rates. Prog Photovolt Res Appl 2016;24:978–89. https://doi.org/10.1002/pip.2744.
[113] Fu R, Feldman D, Margolis R. U.S. Solar photovoltaic system cost benchmark: Q1 2018. Report. National Renewable Energy Laboratory; 2018. https://www.nrel.gov/docs/fy19osti/72399.pdf.
[114] U.S. Department of the Treasury Internal Revenue Service. How to depreciate property. Report. U.S. Department of the Treasury - Internal Revenue Service; 2018. https://www.irs.gov/forms-pubs/about-publication-946.
[115] Feldman D, Bolinger M. On the path to SunShot: emerging opportunities and challenges in financing solar. Report. National Renewable Energy Laboratory and Lawrence Berkeley National Laboratory; 2016. https://www.nrel.gov/docs/fy16osti/65638.pdf.
[116] Cole W, Frew B, Gagnon P, Richards J, Sun Y, Zuboy J, Woodhouse M, Margolis R. SunShot 2030 for photovoltaics (PV): envisioning a low-cost PV future. Report. National Renewable Energy Laboratory; 2017. https://www.nrel.gov/docs/fy17osti/68105.pdf.
[117] Interagency Working Group on Social Cost of Greenhouse Gases - United States Government. Technical support document: technical update of the social cost of carbon for regulatory impact analysis under executive order 12866. Report. Interagency Working Group on Social Cost of Greenhouse Gases; 2016. https://19january2017snapshot.epa.gov/sites/production/files/2016-12/documents/sc_co2_tsd_august_2016.pdf.
[118] Rogelj J, McCollum DL, Reisinger A, Meinshausen M, Riahi K. Probabilistic cost estimates for climate change mitigation. Nature 2013;493:79–83. https://doi.org/10.1038/nature11787.

[119] Van Den Bergh JC, Botzen WJ. A lower bound to the social cost of CO_2 emissions. Nat Clim Chang 2014;4:253–8. https://doi.org/10.1038/nclimate2135.
[120] Moore FC, Diaz DB. Temperature impacts on economic growth warrant stringent mitigation policy. Nat Clim Chang 2015;5:127–31. https://doi.org/10.1038/nclimate2481.
[121] Cai Y, Lenton TM, Lontzek TS. Risk of multiple interacting tipping points should encourage rapid CO2 emission reduction. Nat Clim Chang 2016;6:520–5. https://doi.org/10.1038/nclimate2964.
[122] Nordhaus WD. Revisiting the social cost of carbon. Proc Natl Acad Sci 2017;114:1518–23. https://doi.org/10.1073/pnas.1609244114.
[123] Ricke K, Drouet L, Caldeira K, Tavoni M. Country-level social cost of carbon. Nat Clim Chang 2018;8:895–900. https://doi.org/10.1038/s41558-018-0282-y.
[124] Database of State Incentives for Renewables and Efficiency. Business energy investment tax credit (ITC). http://programs.dsireusa.org/system/program/detail/658; 2018.
[125] US Environmental Protection Agency. Documentation for EPA's power sector modeling platform v6: using the integrated planning model. 2018. https://www.epa.gov/sites/production/files/2018-05/documents/epa_platform_v6_documentation_-_all_chapters_v15_may_31_10-30_am.pdf.
[126] Ondraczek J, Komendantova N, Patt A. WACC the dog: the effect of financing costs on the levelized cost of solar PV power. Renew Energy 2015;75:888–98. https://doi.org/10.1016/j.renene.2014.10.053.
[127] Steffen B. Estimating the cost of capital for renewable energy projects. SSRN Electronic Journal 2019:0–39. https://doi.org/10.2139/ssrn.3373905.
[128] National Renewable Energy Laboratory. Annual technology baseline: electricity. https://atb.nrel.gov/electricity/2019/data.html; 2019.
[129] MIT Energy Initiative. Utility of the future. Report. Cambridge, MA: Massachusetts Institute of Technology; 2016. https://energy.mit.edu/uof.
[130] Taylor JA, Dhople SV, Callaway DS. Power systems without fuel. Renew Sustain Energy Rev 2016;57:1322–36. https://doi.org/10.1016/j.rser.2015.12.083.
[131] Milligan M, Frew BA, Bloom A, Ela E, Botterud A, Townsend A, Levin T. Wholesale electricity market design with increasing levels of renewable generation: revenue sufficiency and long-term reliability. Electr J 2016;29:26–38. https://doi.org/10.1016/j.tej.2016.02.005.
[132] U.S. Energy Information Administration. Henry Hub natural gas spot price. https://www.eia.gov/dnav/ng/hist/rngwhhdA.htm; 2018.